

Rochester Institute of Technology

RIT Digital Institutional Repository

Theses

1988

Measurement of the thermal conductivity of thin solid films with a thermal comparator

Charles A. Amsden

Follow this and additional works at: <https://repository.rit.edu/theses>

Recommended Citation

Amsden, Charles A., "Measurement of the thermal conductivity of thin solid films with a thermal comparator" (1988). Thesis. Rochester Institute of Technology. Accessed from

This Thesis is brought to you for free and open access by the RIT Libraries. For more information, please contact repository@rit.edu.

MEASUREMENT OF THE THERMAL CONDUCTIVITY
OF THIN SOLID FILMS
WITH A THERMAL COMPARATOR

by
Charles A. Amsden

A Thesis Submitted
in
Partial Fulfillment
of the
Requirements for the Degree of
MASTER OF SCIENCE
in
Mechanical Engineering
at
Rochester Institute of Technology

Approved by:

Dr. J. S. Torok

Dr. Joseph S. Torok, Thesis Advisor
Mechanical Engineering Department
Rochester Institute of Technology

Stephen D. Jacobs

Dr. Stephen D. Jacobs, Senior Scientist
Laboratory for Laser Energetics
University of Rochester

Alan H. Nye

Dr. Alan H. Nye, Faculty Member
Mechanical Engineering Department
Rochester Institute of Technology

Alan B. Entenberg

Dr. Alan B. Entenberg, Faculty Member
Physics Department
Rochester Institute of Technology

B. V. Karlekar

Dr. Bhalechandra V. Karlekar, Head
Mechanical Engineering Department
Rochester Institute of Technology

I, Charles Amsden, do hereby grant permission to Wallace Memorial Library, of R.I.T., to reproduce my thesis in whole or in part. Any reproduction will not be used for commercial use or profit.

Charles A. Amsden

Abstract

A direct-reading thermal comparator was used to measure the thermal conductivities of several thin solid films. This new application of the thermal comparator was based on heat flow modelling using the thermal constriction resistance, generalized here for the case of a film on the surface of an infinite half-space.

Four dielectric optical coating materials were tested, and found to have thermal conductivities significantly lower than those for the same material in bulk form.

The finite element method was used to estimate the minimum sample dimensions required for accurate results, and the variation of the thermal constriction resistance with the assumed mode of heat flow between the comparator probe tip and the test specimen.

TABLE OF CONTENTS

1.0 INTRODUCTION	1
1.1 The importance of thin film thermal conductivity	1
1.2 Previous experimental work	1
1.3 Overview of the use of the thermal comparator to measure the thermal conductivity of thin solid films	3
2.0 THE THERMAL COMPARATOR TECHNIQUE	4
2.1 The two ball thermal comparator	4
2.1.1 Early development of the technique	4
2.1.2 Special considerations and effects	6
2.1.3 Applications	8
2.1.4 Previous theoretical modelling	8
2.2 The direct reading thermal comparator	10
2.2.1 Commercial apparatus	10
2.2.2 Additional experimental apparatus	13
2.2.3 Curvefitting	16
2.2.4 Heat flow modelling	17
2.2.5 Determination of the film thickness, substrate conductivity, and heat flow radius	21
2.2.6 Specimen hardness considerations	23
2.3 Results	24
2.4 Discussion of results, and verification of modelling	26
3.0 FINITE ELEMENT ANALYSIS	28
3.1 Motivation and formulation	28
3.2 Results	30
3.2.1 Axisymmetric heat flow problem	30
3.2.2 Effect of domain size on contact temperature	30
3.2.3 Heat flux profile analysis	32
3.3 Summary	34
4.0 CONCLUSION	35
REFERENCES	37
ACKNOWLEDGEMENT	40
APPENDICES	41
I. Curvefitting	41
II. Rootfinding	48
III. Contact Stress Analysis	56
IV. Finite Element Modelling	59
V. Derivation of the Thermal Constriction Resistance	83

FIGURES

2.1	The two ball thermal comparator	4
2.2	Thermal conductivity as a function of differential voltage	6
2.3	Domain of Clark's problem	9
2.4	The direct reading thermal comparator	11
2.5	Apparatus	13
2.6	2-D heat flow model domain	18
2.7	Photograph of the probe tip	22
2.8	Output millivoltage as a function of the applied load	23
2.9	Thermal conductivity of titania films	26
3.1	FEA domain	28
3.2	Axisymmetric temperature distributions	30
3.3	Temperature as a function of sample dimensions	31
II.1	2-D model function	49
III.1	Contact stress local geometry	56
III.2	Probe contact radius	58
III.3	Probe indentation	58
IV.1	FEA domain	59
IV.2	Shape functions	61
IV.3	Coordinate transformation	62
IV.4	Element classification	64
IV.5	Program map	66
V.1	TCR derivation domain	83

TABLES

2.1	Thermal conductivity of optical thin film materials	25
3.1	Variation of thermal constriction resistance with heat flux profile	33
II.1	Film conductivity as a function of normalized thickness and apparent conductivity	49

1.0 INTRODUCTION

1.1 The importance of thin film thermal conductivity

In 1984, it was shown that the thermal conductivity of many thin film optical materials may be much lower than corresponding bulk materials [7]. This has important implications in thermal transport modelling, prediction of the growth and nucleation of thin films, and in their thermal aging and deterioration characteristics. Gross inaccuracies may occur if bulk conductivity data is used to predict conduction through the film. This is especially important in film applications involving a high heat load, such as microelectronics and laser optics. The build up of heat may cause catastrophic failure of the coated device.

Optical coatings, used to enhance the transmissivity or reflectivity of the optic, are susceptible to damage in high power laser applications. Often, sufficient energy is absorbed to burn a hole through the coating. Many people in the optics industry have postulated that there may be a connection between the thermal conductivity and the damage threshold of optical coatings [24]. Low thermal conductivity may cause localized hot spots, and eventual coating destruction. At this point in time, the thermal conductivity of only a few thin film coating materials are known. Further study in this area may result in coatings more suited to high power laser applications.

1.2 Previous experimental work.

Over the past two decades, many experiments have been developed in an effort to accurately measure the thermal conductivity of thin films, ie those ranging in thickness from 100 Angstroms to 10 microns. For the most part, they have been limited to a specific type of film (metallic, etc.), or have required special fabrication techniques. At this time, there is no single accepted method of measuring the thermal conductivity of thin films.

The earliest reported methods of measuring thin film thermal conductivity were done in the U.S. in the 1960's and early 1970's [1,2]. They required specialized film preparation, such as a film on a wire, and were limited to films well over a micron thick.

In 1973, Indian physicists Nath and Chopra [3] reported two new techniques. These methods, one transient, and one steady state, were used to measure the thermal conductivity of thermally evaporated copper films over a range of temperatures. They found the thermal conductivity to be strongly dependent upon the film thickness below a certain value, about five microns. Above this thickness, the results by both techniques approximate bulk data. They attribute the thickness dependence of the thinner films to the scattering of electrons at the grain boundaries and surfaces. The temperature dependence they deduced agrees qualitatively with data for bulk materials. The techniques developed by Nath and Chopra are useful for measurements on films greater than 500 Angstroms thick. The methods described are cumbersome, however, and of questionable accuracy [7].

Several other methods were developed during the 1970's [4-6], but they were used to study only metallic films, generally those of gold, bismuth, and copper. None were applied to dielectric thin film materials.

To date, several groups are known to have studied the thermal conductivity of optical thin film materials. The first was done in 1984 by Decker, *et.al* [7], at Naval Weapons Center, China Lake, California. They used a micro-differential calorimetry technique to study two dielectric materials, silica and alumina, deposited by electron beam evaporation and ion beam sputtering. Their measurement was made over a relatively large surface area (one square centimeter) of the film. They showed the first evidence that the thermal conductivity of optical thin film materials may be as much as two orders of magnitude lower than the same material in amorphous, bulk form. This difference is attributed to a large degree of structural disorder, and a corresponding reduction in the phonon mean free path. The technique described was relatively difficult to implement, requiring the placement of a thermocouple between the film and substrate, and was susceptible to large amounts of error if extreme care was not taken to minimize radial conduction and barrier resistances.

Work done in West Germany by Ristau and Ebert [8] in 1986 generally supports Decker's findings. They used an AC calorimetric technique to measure the optical absorbance and thermal conductivity of five dielectric films. All the thermal conductivity values obtained are orders of magnitude lower than the corresponding bulk data. They made measurements over a spot size of 300 microns (diameter). The AC calorimetric method described incorporates a laser to

heat the sample, and an infrared sensor to measure the resulting temperature distribution. Several parameters, including heat flow to the specimen mount, specimen size, and radiation, must be carefully monitored to achieve accurate results with this technique.

1.3 Overview of the use of a thermal comparator to measure the thermal conductivity of films.

The thermal comparator is useful for measurement of the thermal conductivity of films greater than a tenth of a micron thick (1000 Angstroms). The measurement is made over a circular area approximately 360 microns in diameter. This technique is relatively rapid, non-destructive, and can be made on standard (film on substrate geometry) test samples. The method works most efficiently when the film and substrate materials have much different thermal conductivities, although this is often difficult to establish beforehand. For the study of optical materials with low thermal conductivity, the film is generally deposited on a highly conductive substrate, such as single crystal silicon or sapphire.

The technique consists of bringing a heated probe into contact with a cooler test specimen. Once contact is established, the temperature of the probe tip decreases. The magnitude of the temperature drop depends upon the thermal conductivity of the specimen. Heat flow modelling yields the thermal conductivity of a film on the surface of the test specimen.

2.0 THE THERMAL COMPARATOR TECHNIQUE

2.1 The two-ball thermal comparator

2.1.1 Early development of the technique.

The thermal comparator technique was developed in 1957 by R. W. Powell [9], a physicist who worked at The National Physical Laboratory in Great Britain. He continued to work on the technique at The Thermophysical Properties Research Center, Purdue University, until about 1969 [10,11]. The method was a result of Powell's observation of a common phenomenon: the apparent temperature of an object when touched by the hand. For example, when touching two cups, one metal, the other ceramic, each filled with a cool liquid at the same temperature, one feels different apparent temperatures. The metal cup, being highly conductive, appears to be cooler than the ceramic cup. Powell extended this phenomenon to the two-ball thermal comparator, an experiment capable of measuring thermal conductivity of bulk materials.

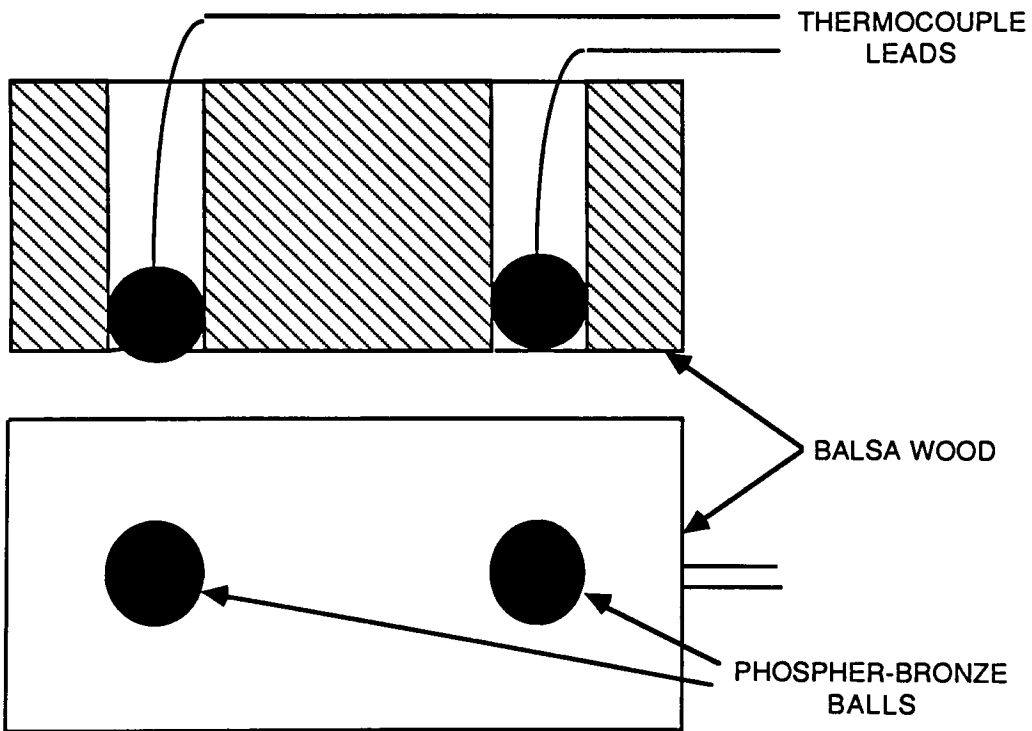
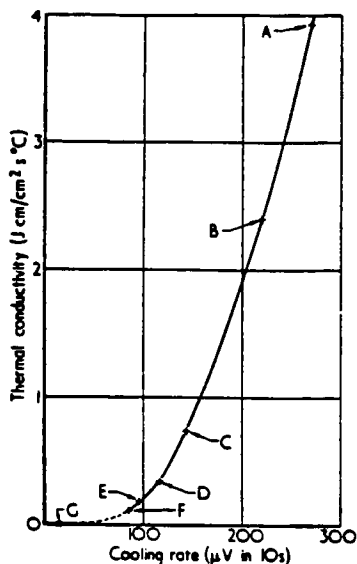


Figure 2.1
Two-ball Thermal Comparator

Powell's two-ball thermal comparator is shown schematically in Figure 2.1. It consisted of a balsa wood block, with two phosphor-bronze balls inserted into cylindrical holes. The balls were positioned such that one protruded slightly from the block, while the other was buried a small amount. Two wires, one constantan, one chromel, were attached to each ball, creating a pair of thermocouples. These wires were then connected to a potentiometer which could measure the differential voltage generated by the thermocouples. The bored holes were stuffed with insulating wool to minimize heat loss.

The experimental procedure was rather time consuming. The whole assembly was placed in an oven, and allowed to reach an equilibrium temperature above ambient. The potentiometer measuring the differential voltage generated by the thermocouples was adjusted to a null condition. Removing the assembly from the oven and bringing it into contact with a specimen caused the temperature of the protruding ball to drop. After a short period of time, a differential voltage was generated by the thermocouples. The magnitude of the differential voltage (temperature) depends upon the thermal conductivity of the specimen. A highly conductive specimen generated a large voltage, while one with low thermal conductivity generated a smaller signal. Samples with a range of known thermal conductivities were measured, and a plot of the conductivity as a function of the generated voltage was made. Measurements made on specimens of unknown conductivity were then compared to the plot to determine their thermal conductivity, hence the name "thermal comparator."

Taking data required a substantial amount of time and careful consideration of many parameters. The apparatus had to reach equilibrium in the oven, at a carefully controlled temperature, between each measurement. The elapsed time between the establishment of contact and the collection of the voltage reading had to be held constant throughout a test run, requiring careful timing.



A, copper; B, aluminium; C, iron; D, alloy steel; E, alumina; F, high alloy steel; G, air.

Figure 2.2
Thermal conductivity as a function of differential voltage

The plot of thermal conductivity as a function of output voltage, shown in Figure 2.2, indicates that the heat flow process may be governed by a power-law or exponential relationship. In his early work, Powell plotted the square root of the thermal conductivity versus voltage, and made two linear fits to the data, one for the low end, the other for the high end of the plot. Later, he switched to a semi-logarithmic plot, and fit a single straight line.

2.1.2 Special considerations and effects

Between 1957 and 1969, a considerable effort was made by Powell and others to determine both the accuracy and applicability of the technique. The technique proved useful for measuring the thermal conductivity of a wide range of materials, but several parameters had to be considered to ensure accurate results. They included: matching the contact resistance between the test samples and the standards, maintaining a constant temperature differential for each test, and the use of high quality standards (of known thermal conductivity).

The thermal contact resistance depends strongly upon the actual area in physical contact between the comparator and test specimen. Several factors have an effect upon this contact area. Most notably, these are the hardness of the materials, the force exerted on the parts, and their surface finishes. In order to match the contact resistance, the standards and the samples must be physically similar. If, for example, the standards are much softer than the samples, the contact area will be

greater for the standards, resulting in a larger temperature drop. This leads to low estimates of thermal conductivity for the test samples. In a similar manner, if the test samples have a better surface finish than the standards, better contact will be made, resulting in high estimates of thermal conductivity. Increasing the applied force increases the deformation of the parts (deformation is directly proportional to the cube root of the applied load [12]), and therefore the contact area and the estimated conductivity. Consequently, the applied force must be kept constant throughout a test run.

Using the same initial temperature is absolutely essential for a valid comparison. Each curve made for a set of standards is only valid for the temperature and force at which the readings were taken. Because the generated voltage depends upon the temperature differential established, slight differences in initial temperature can have a profound effect upon the results. In addition, all samples must be of sufficient size that their temperature doesn't rise significantly during the test. Powell made an effort to determine the minimum size of test specimens to ensure accurate results. However, his work in this area cannot be applied to the present comparator design, due to the large difference in probe radii between the two designs.

The comparator technique is based on comparing samples of unknown conductivity to those of known conductivity. This comparison is only valid if the thermal conductivities of the standards are known to be accurate. In addition, the quality of the standards must be maintained. Many materials, especially high conductivity metals, develop a surface finish (oxidize) over time. This can lead to error if care is not exercised to maintain them.

Ginnings [14], of the National Bureau of Standards, analyzed the two-ball thermal comparator in 1962. He considered the effects of diffusion (time dependence), radiation, gaseous conduction, and solid conduction. He found the transient effects involving thermal diffusion to be of relatively short duration, less than a second. The maximum radiation near room temperature was found to be roughly an order of magnitude smaller than conduction through air. For low conductivity specimens, heat transfer due to gaseous conduction was found to be significant. This could be minimized by increasing the contact area. For moderate to high conductivity specimens, heat transfer was attributed primarily to conduction through solids. In addition, Ginnings recommended that future comparators be

designed to produce constant deformation, rather than apply constant load. This would maintain a constant contact area for all test specimens, and a higher degree of accuracy. Unfortunately, this recommendation was not implemented on later designs. Ginnings attempted to determine an overall relationship between the voltage generated and the specimen thermal conductivity. This relationship was found to be very complex, being a function of many heat transfer processes. Neither a power-law nor an exponential function adequately describes the heat flow process.

2.1.3 Applications.

During the 1960's the two-ball comparator was used to measure the thermal conductivity of a wide range of materials, including a variety of solids, liquids and gases [11]. Nearly thirty papers were published worldwide, noting new applications of the technique. Some of the more interesting were *in vivo* measurements made on animal bones at Auburn University, and measurements made on fruits and fruits and vegetables, with the use of a plastic membrane. The method was also used extensively in Australia to rapidly identify various gemstones in their natural environment.

The determination of the thermal conductivity of liquids and gases was accomplished by using a shallow dish to contain the fluid. The dish was covered by a tightly stretched plastic material, such as Melinex. The comparator was then brought in contact with the surface of the membrane, and readings were taken in the usual way. In this case, fluids such as water, glycerin, and carbon tetrachloride were used to generate a calibration curve.

2.1.4 Previous theoretical modelling

W. T. Clark, an associate of Powell at the National Physical Laboratory in Great Britain, theoretically considered conduction through the contact area [15]. As the diameter of the spherical ball was approximately two orders of magnitude larger than the contact diameter, he assumed the sphere to be a semi-infinite solid. He used the center of the contact circle as the origin of the cylindrical coordinate system. The domain is shown in Figure 2.3. It consists of two infinite half-planes. The region $z > 0$ corresponds to the ball; the region $z < 0$ to the specimen. Both regions extend to infinity.

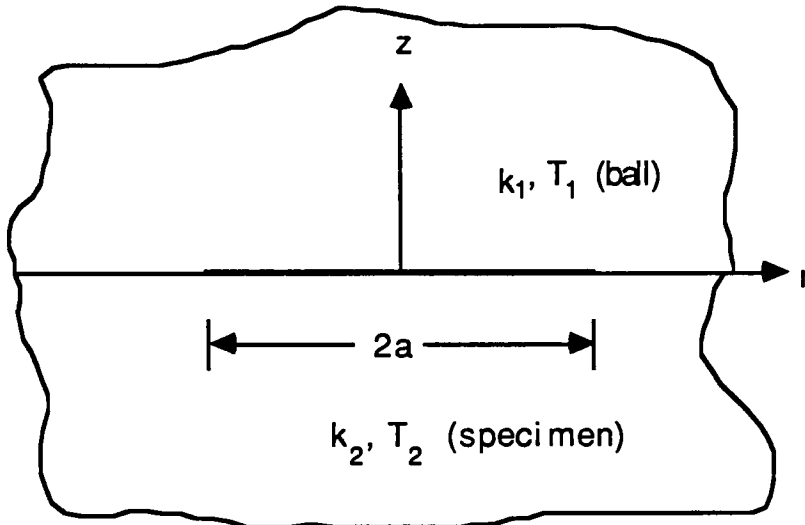


Figure 2.3
Domain of Clark's problem

Considering the comparator to be a steady state device, and assuming axial symmetry, the problem is reduced to two dimensional heat flow in two infinite half-planes with different thermal conductivities. The temperature in each region is governed by Laplace's equation (in cylindrical coordinates).

$$\frac{\partial^2 T}{\partial r^2} + \frac{1}{r} \frac{\partial T}{\partial r} + \frac{\partial^2 T}{\partial z^2} = 0$$

The boundary conditions were prescribed as matched temperature and heat flux over the contact surface ($z=0, r < a$), zero heat flux at $z=0$ outside the radius of contact 'a', zero temperature as 'r' goes to infinity in each region, $T=T_0$ as 'z' goes to plus infinity, and $T=0$ as 'z' goes to minus infinity . The two boundary value problems (one for each region) were then solved with the use of the Hankel transform.

Clark found the temperature of the contact to be independent of the contact radius, and constant over the contact area. This may not hold true if the effect of gaseous conduction in the proximity of the contact is considered as well. The thermal constriction resistance, or resistance to heat flow, was shown to be:

$$R = \frac{k_1 + k_2}{4k_1k_2a} = \frac{1}{4k_1a} + \frac{1}{4k_2a}$$

The thermal constriction resistance for a single infinite half-plane is discussed further in Section 2.2.4 and Appendix V.

The effect of a transient term was considered by including a time dependent term in Laplace's equation. It confirmed the fact that the contribution of a transient term is generally small, much less than ten percent of the steady state term after only ten seconds.

Assuming the film thickness 't' to be much less than the contact radius, Clark considered the effect of an interfacial insulating film on heat flow by adding its contribution to the thermal resistance. If the thermal conductivity of the film is small compared to the specimen conductivity, the dissipation of heat along the film can be ignored, and the thermal constriction resistance becomes:

$$R_T = \frac{1}{4k_1a} + \frac{1}{4k_2a} + \frac{t}{\pi k_3 a^2}$$

where the subscript '3' denotes the film conductivity.

Although he estimated that films as thin as 585 Angstroms could have a measurable effect on the output voltage, there is no literature indicating that Clark's modelling was implemented to measure either the thickness or the thermal conductivity of surface films.

2.2 The direct-reading thermal comparator.

2.2.1 Commercial apparatus.

Although useful, the two-ball thermal comparator suffered several shortcomings. Among the most serious was the long period of time required for the re-establishment of equilibrium temperatures between tests. In 1962, Clark and Powell proposed an alternate, direct reading design [15]. They suggested that it would eliminate the need for accurate timing, and would be less dependent upon surface finish and the elastic properties of the test material. It wasn't until the early 1970's that a direct-reading model was actually built.

Lafayette Instrument Company made a direct-reading thermal comparator available in the mid-1970's [13]. This model, based on Clark and Powell's design, is shown in Figure 2.4. Although still sensitive to material hardness and surface finish, it is capable of taking rapid readings. With the probe maintained at a constant temperature twenty degrees Celsius above ambient, readings may be taken at the rate of about one every thirty seconds, without a measurable drop in the reservoir temperature.

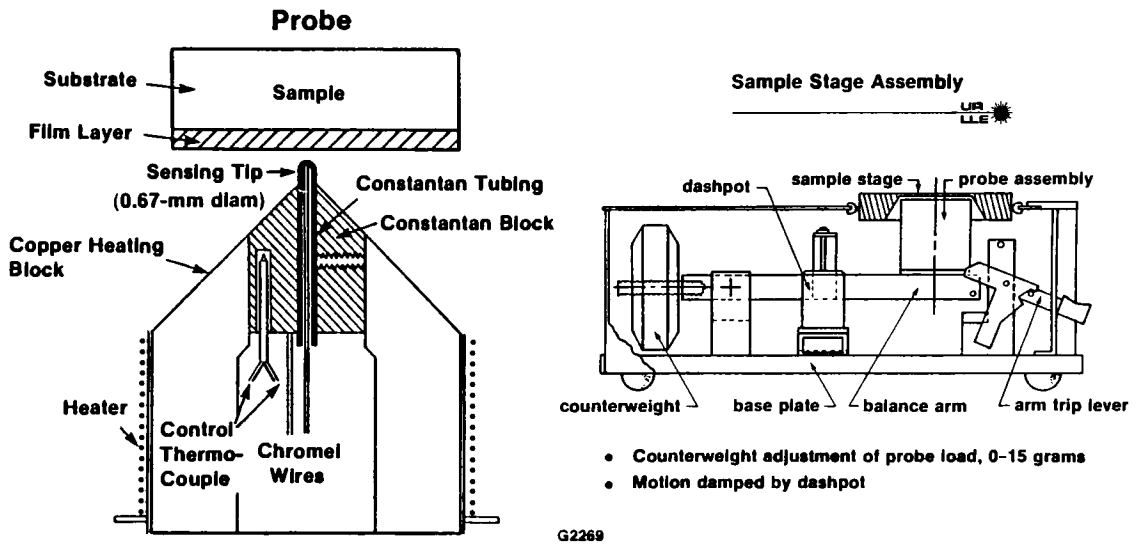


Figure 2.4
The direct-reading thermal comparator

The direct-reading design utilizes a single probe in place of the two phosphor-bronze balls. The probe tip extends from a thermal reservoir made of copper, which is held at a constant temperature above ambient by an electrical resistance heater, connected to a proportional band controller. When the probe tip is brought in contact with a specimen at ambient temperature, the temperature of the tip quickly drops to a steady intermediate value, depending on the thermal conductivity of the specimen. This temperature drop is explicitly given by the equation:

$$(T_1 - T_c) = \frac{k_2(T_1 - T_2)}{(k_1 + k_2)}$$

The subscript '1' refers to probe tip temperature and thermal conductivity, '2' to specimen temperature and thermal conductivity, 'c' to the temperature of the contact. If the temperature of the contact area could be accurately measured, the

thermal conductivity of the specimen could be determined directly. Unfortunately, the only way to accomplish this would be to have the specimen and probe form a thermocouple junction. Except in special circumstances, this is not feasible. Instead, the tip of the commercial unit contains a constantan-chromel thermocouple located within 0.01 inch of the surface, referenced to a similar thermocouple imbedded in the thermal reservoir. The measured temperature difference approximates that of the contact, but a calibration curve of measurements from standards of known conductivity must be used to find the unknown thermal conductivity of a specimen being tested.

The probe tip is shrouded in insulation to minimize heat loss, and mounted on a counter balanced arm supported by bearings, similar to a beam balance. The force exerted by the probe tip on the specimen can be set by adjusting a counterweight. The balance arm is normally held in the down position by a spring loaded trip lever, with the probe tip not in contact with a sample. Pushing the trip lever down allows the balance arm to move upward, its motion damped by a dashpot, until the probe comes in contact with a specimen, oriented face down on a sample stage. A reading is then made. Releasing the trip lever returns the balance arm to the down position.

The differential voltage generated by the thermocouples is sent through a shielded cable to a control and readout module, which contains two subsystems. The first is a voltage amplifier, set at a thousand-to-one gain. This boosts the thermocouple differential voltage from microvolts to millivolts. This signal is then displayed on a digital voltmeter, and sent out of the module for further processing. The other subsystem controls the operation of the heater in the thermal reservoir. A proportional band controller maintains the temperature of the copper reservoir at a value preset by the operator, via an external control knob on the readout module. The heater is capable of maintaining a reservoir temperature thirty degrees Celsius above ambient, but fluctuations in the reservoir temperature produce experimental error. If the temperature is kept about twenty degrees above ambient, the heater and controller are capable of maintaining the reservoir temperature constant to within a tenth of a degree Celsius.

2.2.2 Additional experimental apparatus.

The commercial comparator and control module purchased were designed to test the thermal conductivity of bulk solids and liquids. In an effort to increase the accuracy of the measurements, and the rate at which data could be collected and reduced, several additional items were used. They include a sample enclosure with its own temperature controller, heater and fan, and a personal computer with an on-board analog-to-digital signal converter. A schematic of the apparatus is shown in Figure 2.5.

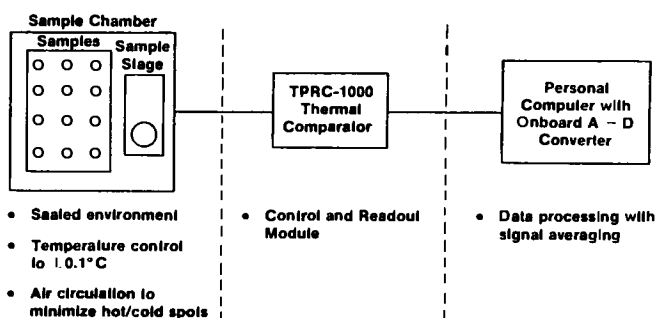


Figure 2.5
Apparatus

The sample enclosure consists of a box, with outer dimensions of approximately 3'x3'x2'. Its walls are constructed of half inch thick plexi-glass, with foam insulation over the outer surfaces. The operator accesses the comparator and test specimens through "glove box" holes on its side. The sample enclosure serves several purposes. First and foremost, it controls the temperature the test specimens. In addition, it helps maintain the cleanliness and quality of the test specimens.

The enclosure was built in 1984, as part of an early effort at The Laboratory for Laser Energetics (LLE) to determine the feasibility of using the thermal comparator to measure thin film thermal conductivity. At that time, the temperature of the samples was controlled by placing them on a heated brass plate inside the enclosure. Two temperature controllers were used, one to maintain the temperature of the brass plate, the other to maintain the temperature of the air enclosed. Each controller had its own strip heater. One heater was located inside the top of the

enclosure, the other under the brass plate. The only temperature readout available was from the comparator control module, which measured the ambient air temperature of the enclosure. The temperature of the brass plate, maintained by its own controller, was not monitored. At that time, the air in the enclosure was not circulated, resulting in large temperature gradients. The air near the top surface was much warmer than the brass plate, located on the bottom of the enclosure. With the set point of the two controllers adjusted to the same temperature, the heater and sensor located under the brass plate effectively controlled the temperature of the whole enclosure, as the warm air near the air temperature sensor prevented that system from engaging.

During the Summer of 1987, the enclosure temperature system was switched to forced air convection, in an effort to more closely monitor and maintain the temperature of the specimens. A single 480 Watt strip heater was mounted on standoffs against the back wall of the enclosure. A fan was installed to eliminate hot spots, and circulate the air past a thermistor probe, which was used by a single temperature controller (located outside the enclosure) to maintain the air temperature in the enclosure to within a tenth of a degree Celsius.

In addition to providing a means of temperature control, the enclosure also helps maintain the quality and cleanliness of the test specimens. Desiccant packs line the box to reduce the humidity of the air enclosed, thus slowing degradation of the metal standards. Operators wear surgical gloves while taking data to minimize the transfer of perspiration and other contaminants to the enclosure and test specimens. The temperature inside the enclosure is maintained at near that of the human body (35 degrees Celsius) to prevent the operators arms and hands from heating the air.

All specimens are cleaned thoroughly before they are placed in the enclosure. To prevent damage to their surfaces, surgical gloves are worn while handling them, and all surfaces within the enclosure that may come in contact with the specimens are coated with Teflon, chosen for its softness and stability. Often, items placed in contact with Teflon have a tendency to develop a static charge. In an effort to reduce this, all items in the enclosure, including the operator's arms, are grounded.

Computer averaging of the output voltage signal was implemented in an effort to increase the accuracy and repeatability of the measurements. When the probe tip

is brought in contact with a specimen, the voltage reading reaches a relatively steady value, but still may fluctuate by one to two percent. Initially, a waveform analyzer was installed to convert the analog voltage to a digital value, and average the output voltage over a period of ten seconds. The average value was then sent to a personal computer for storage in a data file. Later, an onboard analog-to-digital converter was installed on the computer, freeing the waveform analyzer for use on another experiment. The personal computer takes two readings per second, over a period of ten seconds, and computes the mean and standard deviation of the values. If the standard deviation is less than two percent of the mean value, the mean value is placed in a data file determined by the operator.

At the end of a data run (3-5 readings per specimen), the computer is used to calculate and print the average and standard deviation of the readings in each file. The standard deviation is an indication of how repeatable the readings were during the run, and sometimes varies considerably from material to material.

A concerted effort was made to increase the repeatability of measurements. Many parameters were investigated. Several were found to have a significant effect, including: the cleanliness of the enclosure, the force exerted by the probe on the sample while a reading is taken, the location of the control module (outside the enclosure), and the temperature of the probe (above ambient).

The cleanliness of the enclosure, as mentioned earlier, must be maintained. Although the operators wear surgical gloves, often their forearms are exposed. Chafing of the access covers has a tendency to remove a considerable amount of skin and hair. Two courses of action can be taken to control the problem: either the enclosure must be cleaned on a regular basis, or the operator's must wear longer gloves, which cover their forearms.

Increasing the probe force on the sample tends to enhance the quality of the contact, and reduce the standard deviation of the readings taken. Unfortunately, it also increases the deformation of the samples (discussed further in Section 2.2.6). Caution must be exercised in increasing the probe force to increase accuracy and repeatability.

The location of the comparator control module can have a significant effect on the repeatability of results. It seems that it is susceptible to electromagnetic

interference. At the present time, it is kept on top of the enclosure, distant from the temperature controller and fan transformer.

During early work at LLE, the thermal reservoir in the probe tip was kept at as high a temperature possible above ambient (about 30 degrees Celsius), to get the widest possible spread of voltage readings. The probe heater and controller were not capable of maintaining this temperature difference throughout a data run, and the temperature of the thermal reservoir often dropped. The reservoir is now kept about twenty degrees Celsius above ambient, so that its temperature can be held constant throughout a test run, increasing repeatability.

Taking these considerations, the voltage readings taken seldom fluctuate by more than five percent. Higher fluctuations may be partially attributable to local variations in the thermal conductivity of the test samples. An (optical type) iris has occasionally been used to center the test samples, in an effort to check for local variations, but the result of these efforts have been inconclusive to date.

2.2.3 Curvefitting

Once data is taken on a set of standards and test specimens, curvefitting is required to find the thermal conductivity of the test specimens. The particular commercial comparator that was used came with a calibration curve for a probe twenty degrees Celsius above ambient. As small changes in the probe temperature can result in substantial shifts in the calibration curve, the manufacturer recommends that a calibration curve be generated for each test run. Initially, this was done by hand, using a french curve to fit the standard data plotted on semi-logarithmic paper. In an effort to make the process more systematic, the process is now done numerically, using a VAX 11-750 computer. Several methods were tested, and compared to manual plots in an attempt to determine their relative merits.

The first numerical technique tried was a least squares fit [26], using a linear sum of four functions. In fitting the curve, the computer determines a coefficient, or scale factor, for each function. Various combinations of polynomial and exponential functions were tried; none met with success. The magnitude of the coefficients varied widely, and alternated in sign, resulting in tremendous computer error when the difference of two functions was taken. This technique was judged unacceptable, at least for these functional forms.

A linear least squares fit was then made to the exponential of the known conductivity as a function of the voltage, emulating the semi-logarithmic plot used by the manufacturer. This fit the data reasonably well, but over a period of time, a trend was observed. The data for each standard always seemed to fall at a particular location with respect to the curve, on one side or the other. As there is no theoretical basis for the purely exponential relationship (and linear fit), a cubic spline interpolation routine was written. A visual comparison of k vs. V and the exponential of k vs. V was made, the latter resulting in what seemed to be a better fit. This is the method used at present. The FORTRAN program written is shown in Appendix I.

The cubic spline interpolation technique has one significant limitation. It cannot be used to extrapolate values outside the conductivity range established by the standards. This has caused some problems in testing films of relatively high thermal conductivity on similar substrates. The voltage value obtained, higher than our highest standard, cannot be compared to determine its apparent conductivity.

Berilco copper was used for several years as a high conductivity standard, but it had a tendency to oxidize very quickly, requiring frequent repolishing. Both gold and synthetic diamond have been considered as stable, high conductivity standards. A finite element program was implemented in an effort to numerically estimate the minimum size required for accurate measurements. Section 3.2.2 contains the results of this effort, and a discussion. To date, no high conductivity standard has been purchased to replace copper.

2.2.4 Heat flow modelling

The thermal comparator technique is useful for making thermal conductivity measurements on bulk materials. When a highly conductive specimen, coated with an insulating film is tested, the comparator indicates a reduction in the apparent conductivity of the specimen. Modelling is required to extract the film conductivity from the apparent conductivity measured by the apparatus.

As an initial approximation, a one-dimensional heat flow model was developed by the Mechanical Engineering Department of the University of Rochester [25]. Several assumptions were made, including one-dimensional heat flow from the probe tip through both the film and the substrate (considered to be of finite

thickness), with no time dependence. These assumptions severely limited the accuracy of the model. In an effort to rectify this, a two-dimensional model is developed here.

The model developed is similar in some respects to Clark's model, discussed in Section 2.1.4. Heat flow is assumed to be axially symmetric, with no time dependence, into an infinite half-plane. Several important differences exist, however. The probe tip is not included, reducing the domain to a single infinite half plane. In addition, no assumptions are made about the relative sizes of the heat flow radius and film thickness.

The model consists of relating two definitions of the thermal constriction resistance, one developed for the case of no film, the other for the presence of a film.

Carslaw and Jaeger were the first to define the thermal constriction resistance. It is defined as "the thermal resistance to steady heat flow from a circle of radius 'a' into a half space", or the ratio of the average surface temperature to the rate of flow of heat [16]. The domain of their problem is shown in Figure 2.6(a).

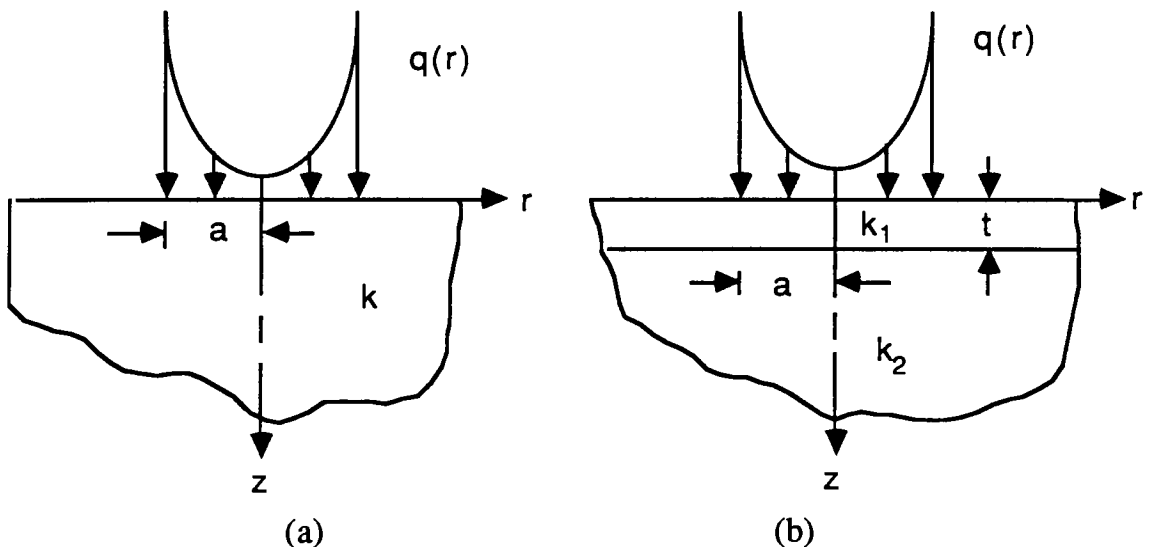


Figure 2.6
2-D heat flow model domain

The heat flux, $q(r)$, assumed to be such that the surface temperature over the heat flow radius 'a' is constant, is given by [17]:

$$q(r) = -k \frac{\partial T}{\partial r} = \frac{Q}{2\pi a \sqrt{a^2 - r^2}}$$

where Q is power (rate of energy transfer). The $z=0$ surface outside the heat flow radius is assumed to be insulated ($q=0$). The assumption of axial symmetry requires that the radial flux across the 'z' axis be zero. The temperature is assumed to go to zero as both 'r' and 'z' go to infinity. If the material has thermal conductivity 'k', the thermal constriction resistance is then defined as [16]:

$$R = \frac{1}{4ka}$$

In 1983, Dryden [17] defined the thermal constriction resistance for the case of a film of thickness 't' on the surface of the specimen, as shown in Figure 2.6(b). The heat flow in each region was assumed to be steady state, governed by Laplace's equation. The boundary conditions were identical to those used by Carslaw and Jaeger, with the addition of matched temperature and heat flux at the film-substrate interface. This formulation resulted in one boundary value problem for heat flow in the film, and one for heat flow in the substrate. These problems were then solved with the use of the Hankel transform. The thermal constriction resistance was shown to be:

$$R = \frac{1}{4k_1 a} + \frac{2}{\pi k_1 a} \sum_{j=1}^{\infty} \left[\theta^j I(\alpha_j) \right]$$

where:

$$\theta = \frac{k_1 - k_2}{k_1 + k_2}$$

$$I(\alpha_j) = -\alpha_j + \left[D - \frac{1}{2D} \right] \sqrt{1 - \frac{1}{D^2}} + \frac{1}{2} \sin^{-1} \left[\frac{1}{D} \right]$$

$$D = \frac{\alpha_j}{2} + \sqrt{\frac{\alpha_j^2}{4} + 1}$$

Knowing the heat flow radius 'a', and the apparent thermal conductivity of a film and substrate combination measured by the thermal comparator, we can define the apparent thermal constriction resistance as:

$$R = \frac{1}{4k_{app} a}$$

This resistance must be equivalent to the form defined by Dryden. Equating the two, and setting the result to zero, gives a function of the substrate conductivity, the apparent conductivity, and the ratio of film thickness to heat flow radius:

$$\frac{1}{4k_1} + \frac{2}{\pi k_1} \left[\sum_{j=1}^{\infty} \theta^j I(\alpha_j) \right] - \frac{1}{4k_{app}} = 0$$

If the film thickness, heat flow radius, and substrate conductivity are known, the equation becomes a function of one variable: the film conductivity. Finding the solution manually is difficult. Therefore, a numerical rootfinding technique is implemented. Summation is stopped when the last term summed is a hundred millionth the first term. If the summation exceeds a million terms without satisfying this criterion, the process is terminated.

Initially, a secant method subroutine was chosen for its rapid convergence characteristics. This method did not meet with success, however, as the function becomes unbounded for low film conductivities (See Appendix II). The method has a tendency to diverge in this area. A less efficient, but more stable technique, the bisection method, was then tested. A special driving program was written specifically to find the root of a monotonically decreasing function. If the solution is not in the initial search range (generally a specified order of magnitude), the program automatically shifts the search range an order of magnitude in the direction of the root. If the solution is not found within a specified number of shifts, the program is terminated. The function converges slowly, especially for small ratios of film thickness to heat flow radius. As many as several thousand summation

terms may be required to meet the convergence criteria specified above. The FORTRAN program, bisection subroutine, and a table of typical film conductivity values are shown in Appendix II.

As the table in Appendix II shows, the model becomes very sensitive when the apparent conductivity measured by the comparator approaches the substrate conductivity. In this range, the presence of noise in the system tends to produce large changes in the output film conductivity values, resulting in potentially large error. The results are most reliable when the film has a much lower conductivity than the substrate. The apparent conductivity is then measurably reduced due to the presence of the film, and potential error due to system noise is minimized.

It should be noted that both forms of the thermal constriction resistance that are used were based on an isothermal flux profile. In reality, the contact spot is almost certainly not isothermal. This may result in experimental error. Section 3.2.3 investigates the effect of the form of the heat flux used on the thermal constriction resistance.

Appendix V shows how the thermal constriction resistance could be defined for the case of multiple films on the surface of an infinite half-plane.

2.2.5 Determination of the film thickness, the substrate conductivity, and the heat flow radius.

The equation relating the apparent constriction resistance to the actual constriction resistance (for a film/substrate combination) is a function of the apparent conductivity (as measured by the comparator), the substrate conductivity, the film conductivity, and the ratio of film thickness to heat flow radius. To solve for the film thermal conductivity, the substrate conductivity, film thickness, and heat flow radius must be specified.

Single crystal silicon or sapphire, with known crystal orientation, are desirable substrate materials. The apparent conductivity of both materials is reduced significantly due to the presence of most optical coatings. In addition, tabulated thermal conductivity values for both materials are readily available for use in the model.

The thickness of the deposited film is generally given by the group who prepared it. They know, that for a given deposition rate, a certain period of time is required to deposit a film of a certain thickness. As an additional measure, the thickness is generally checked using optical or physical techniques.

The radius of the heat flow area between the probe tip and the sample depends upon the geometry of the probe tip, and the probe force used. An associate at LLE used an optical imaging system in an effort to analyze the contact made by our probe. A Helium-Neon laser beam was directed at the contact our probe made with a special aluminum jig, using a probe force equivalent to five grams mass. The jig was designed such that the probe contact was at the same elevation as the bottom of a test sample, duplicating test conditions. The image (silhouette) was focused on a digital image analyzer, and shown on a non-distortion video monitor. The non-contact image of the probe is shown in Figure 2.7(a), the contact image with the jig in 2.7(b). An estimate of the radius through which heat flows was made by comparing the contact diameter to the maximum diameter of the probe (measured with a commercial optical comparator).

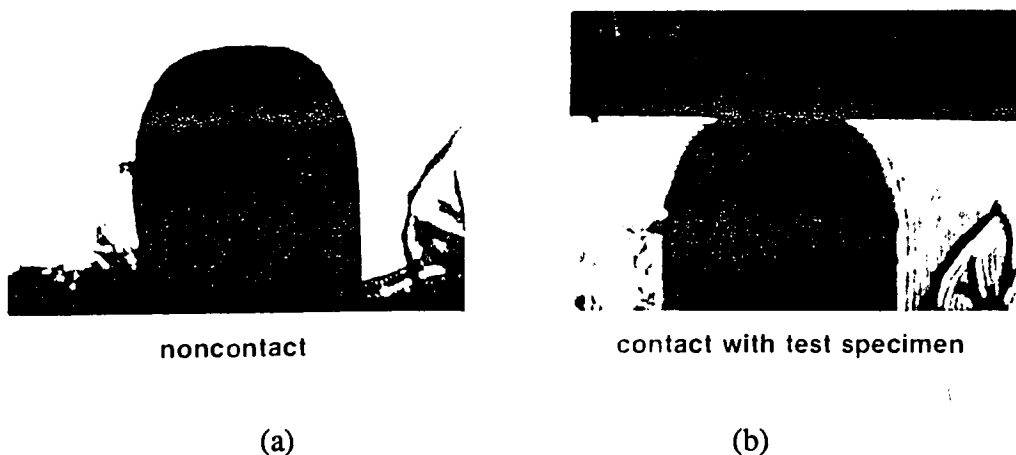


Figure 2.7
Photograph of the probe tip

The actual radius of physical contact, calculated by contact stress analysis and shown in Appendix III, was found to be about one order of magnitude lower, about 20 microns. However, the domed shape of the probe tip brings a large area of its top surface in the proximity of the sample. There is a substantial area in which the probe and sample are separated by a small distance, perhaps one to ten microns.

Convection is occurring in this region. The use of the physical contact radius in the model would be correct only if measurements were taken in a vacuum, with no gaseous conduction. For measurements taken in air, the heat flow radius is assumed to be about 180 microns.

2.2.6 Specimen hardness considerations

An effort was made to determine the effect of increasing the probe force on the output millivoltage readings. A series of measurements were taken on our standards, varying the load from 1.1 to 15 grams. The results of this testing are shown in Figure 2.8.

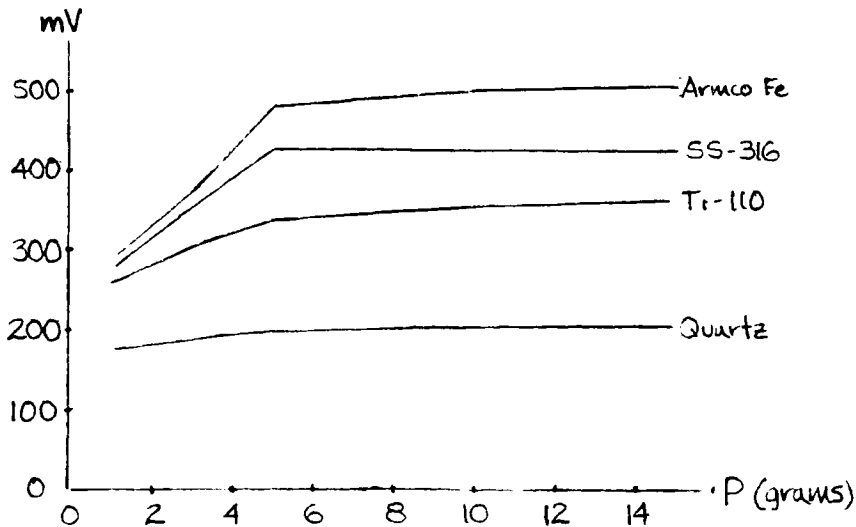


Figure 2.8
Output millivoltage as a function of applied load

Below five grams, the output millivoltage varies with the applied load. This is probably due to variation in the nature of the contact, and therefore the contact resistance. The millivoltage readings are relatively constant above five grams. This indicates that, for fairly hard materials, such as our standards, the contact resistance between the probe tip and specimen is essentially constant, as long as at least five grams are applied.

Testing at or above five grams presents no problems with hard films. In fact, the higher load seems to reduce the noise in the readings taken. There are potential problems, however, in testing softer films at this load. Five grams may be enough to significantly deform the film. For this reason, it may be wise to test softer films at a lower load, perhaps 3.5 grams. This would reduce the film deformation. It

must be recognized that, due to differences in the contact resistance, there is a potential for error when soft film data is fit to a calibration curve generated by harder standards, even though all are tested at the same load. Appendix III contains deformation and indentation calculations for materials in the range of interest.

One of the most significant results of the variable load testing is the non-zero intercept on all the curves. If the heat were flowing only through the area of physical contact between the probe and sample, all the plots would have zero intercepts. As the load is reduced to zero, the contact area becomes a point, with zero heat flow. The non-zero intercept on the plots verifies the fact that convection is occurring outside the region of physical contact.

2.3 Results

Table 2.1 shows the results of testing through December 1987. All the data shown is for films deposited on single crystal silicon with a crystal orientation of (111).

TABLE 2.1

Thermal Conductivity of Optical Thin Film Materials (W/mK)*

	t (μm)					Ristau ⁸	Decker ⁷	Bulk	Test Load ^c	Notes
	0.5	1.0	1.5	2.0	4.0					
SiO ₂ [†]								1.2 ¹⁸ - 10.7 ¹⁹		
IBS	.21	.18		.21	.39		.28 (t=.5μm)			5g, 10 g
EBE	.14	.18		.24	.40	.10(t=1μm)	.17(t=1μm)		5 g	a
TiO ₂ [†]								7.4-10.4 ²⁰		
IBS	.16	.20		.29	.37				5g, 10 g	
EBE	-.07	.12	-.15	.21		.018(t=1μm)			5 g	a
MgF ₂ [†]								14.6 ¹⁸ - 30 ²¹		
IBS	.12	.33			.52				3.5 g	
EBE	-.31	-.26							3.5 g	b
Al ₂ O ₃ ^{††}								20 ⁷ - 46 ²⁰		
EBE	-.16			-.27	-.34		.25(t=1μm)		5 g	

* Estimated uncertainty ± 10% except those indicated (-), which may vary 20-50%.

† Samples provided by Optical Coating Laboratory, Inc., Santa Rosa, CA.

†† Samples provided by the Thin Film Coating Facility of the Institute of Optics, University of Rochester.

a Some samples crazed, no distinct difference between crazed and uncrazed measurements.

b All samples crazed.

c Results relatively independent of load for hard films. For soft films, data for lowest load is

Figure 2.9 shows the thermal conductivity of titania films as a function of their thickness. The standard deviation of six data runs are represented by error bars. The thinner films, supplied by Air Force Weapons Lab (Kirtland Air Force Base, Albuquerque, NM), were deposited on sapphire substrates. The thicker films, prepared by Optical Coating Laboratory, Inc. (Santa Rosa, CA), were prepared on silicon substrates.

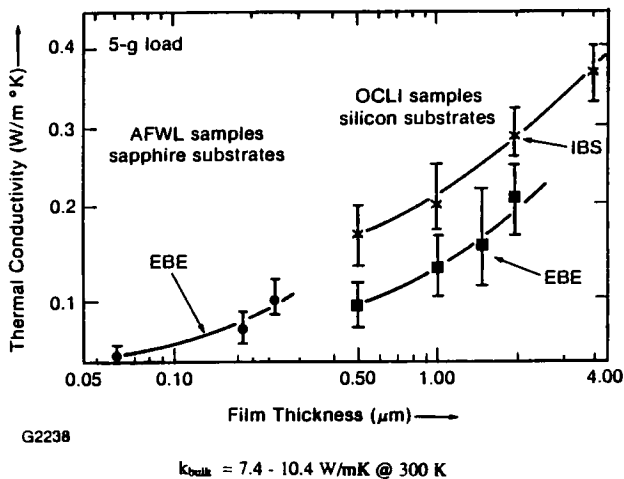


Figure 2.9
Thermal Conductivity of TiO₂ Films

2.4 Discussion of results

In Figure 2.9, the two curves representing electron beam evaporated films are slightly misaligned. This may be due to differences in film deposition parameters (for example, the temperature of the substrate during deposition). In light of the large difference in apparent conductivities measured by the comparator, the curves seem to verify the validity of the heat flow model used to extract the film data. A single curve could be fit to all the points corresponding to evaporated films, and lie within the error bars.

The data represented in Figure 2.9 also indicates that titania films deposited by sputtering have a higher thermal conductivity than those deposited by evaporation. This difference is not apparent for other materials, such as silica and magnesium fluoride.

Virtually all the results to date indicate that the thermal conductivity of dielectric thin films increases with increasing film thickness. There are several plausible explanations for this phenomenon. The most obvious is that the percentage crystallinity of the films may be changing with thickness as the film is grown. The material in close contact with the substrate may be more disordered than the material further away from the interface. The change in crystallinity could be the result of substrate heating as material "condenses" on the surface during deposition. The variation in conductivity with distance from the interface would result in higher net thermal conductivities for thicker films than thin ones.

Another possible explanation is localized dislocation between the film and substrate at the interface. This would create a thin layer of air between the film and substrate, a barrier to heat flow. The effect of this localized peeling would be more apparent for thinner films than thick ones. This explanation seems particularly valid for evaporated films, known to have high levels of tensile stress and a propensity for crazing. It should be noted that the thermal conductivity of evaporated titania films approaches that of air as the films become very thin.

It should be noted that the variation in thermal conductivity with thin film thickness was noted in the past. In their studies of copper films in 1976, Nath and Chopra [3] noted that the thermal conductivity of copper films varied with thickness below five microns.

3.0 FINITE ELEMENT ANALYSIS

3.1 Motivation and formulation

Finite element analysis was performed with several goals in mind. Initially, it seemed to be a method of extracting the thermal conductivity of a single film in a multilayer stack from the apparent conductivity read by the thermal comparator. It also promised to provide information about sample size requirements, and the accuracy of the analytical model used to reduce single film data.

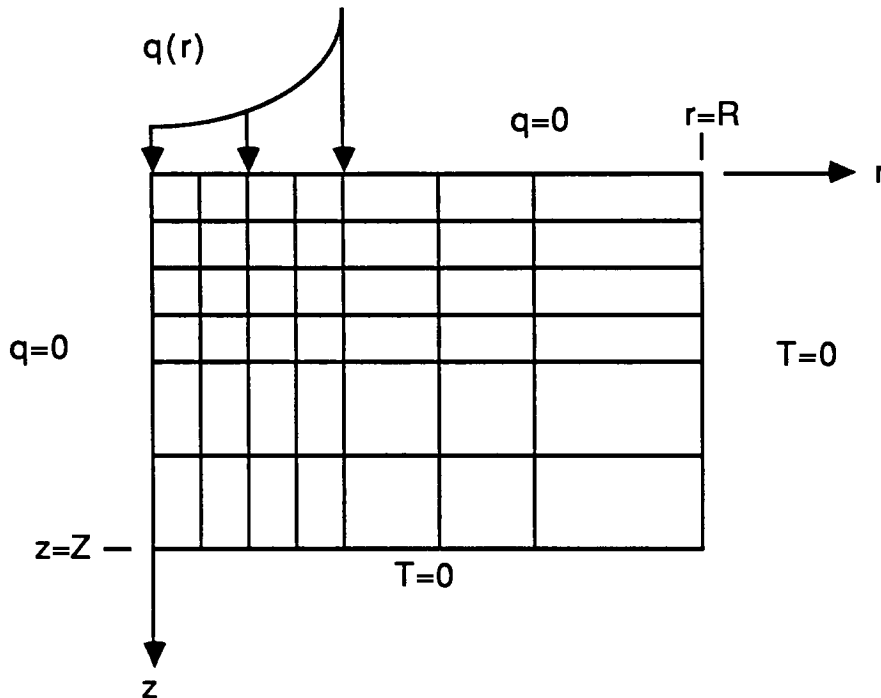


Figure 3.1
FEA domain

The problem formulation is based on the domain and boundary conditions shown in Figure 3.1. The domain is very similar to that of Figure 2.6, with one significant exception: it doesn't extend to infinity in the 'r' and 'z' directions. Using cylindrical coordinates, symmetry about the z-axis reduces a three dimensional region to two dimensions. Heat flow is assumed to be steady, governed by Laplace's equation. The temperature is specified on two boundaries, the heat flux is specified on the other two.

Four noded, rectangular shape functions were used in the derivation of the equations. The thermal conductivity was assumed to be constant over each element, but allowed to vary between elements, as specified by the user. The 'r' and 'z' coordinates of the element boundaries, and the heat flux function $q(r)$ are user specified. The complete formulation and program package are shown in Appendix IV.

Given the heat flux function $q(r)$, and the thermal conductivity of each element, the program package solves for the temperature at each node. A contour plotting package developed by The National Center for Atmospheric Research (NCAR) is used to plot isotherms in the region.

The model has three key parameters: the power input (specified in the heat flux function), the thermal conductivity of each element, and the temperature of the contact at $z=0$. Given any two of the three, the program is capable of finding the third. The temperature of the contact can be found with one program execution. Solving for the power input or thermal conductivity requires multiple program executions, with suitable parameter modifications between iterations.

Although successful in other ways, the finite element model developed is not useful for reducing the results of tests on multilayer stacks. The comparator apparatus provides too little information. Solving for an unknown conductivity would require the power input and contact temperature to be known. The power can be found from the apparent conductivity, contact temperature, and heat flow radius 'a' using the equation [16]:

$$Q = 4k_{app} T_c a$$

The problem lies with estimating the contact temperature. Because it is located approximately 0.030 inch from the surface, the thermocouple located in the comparator probe tip does not measure the temperature of the contact, but the temperature of a location near the contact. The temperature gradient in this region is steep. Using the temperature registered by the thermocouple in the model could potentially result in large error.

3.2 Results

3.2.1 Axisymmetric heat flow problem.

As a test of the analysis package and plotting routine, a simple problem was examined. The problem consisted of heat flow into a 'square' domain (actually a cylinder with radius equal to thickness). A constant temperature flux profile was assumed, with heat flowing into the $z=0$ surface. Several runs were executed, varying the number of nodes in each direction, and varying the thermal conductivity.

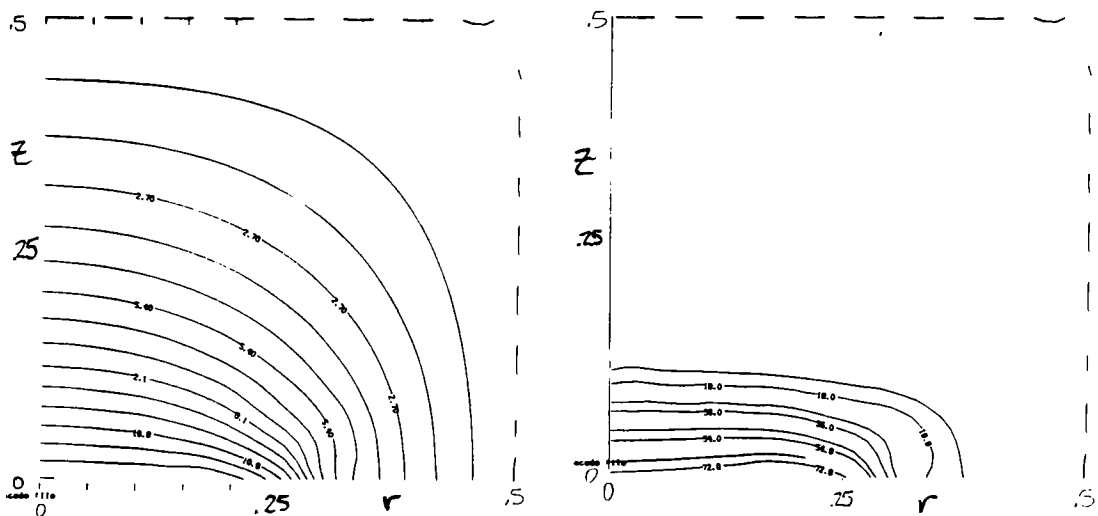


Figure 3.2
Axisymmetric temperature distributions

Isotherm contour plots for two cases are shown in Figure 3.2. Case 1 shows the isotherms for a material of constant thermal conductivity, while Case 2 shows the effect of an insulating layer on the surface.

As expected, the number of nodes (elements used) had no effect on the solution. The temperature was found to be fairly constant over the flux surface, and the isotherms are normal to the surface at the zero flux borders.

3.2.2 Effect of domain size on contact temperature

The thermal comparator technique requires that the samples tested be fairly large compared to the contact radius. If the dimensions of the sample are too

small, the exposed back or side surfaces of the sample will heat up, resulting in convective heat transfer, and invalid comparisons.

The analysis package was used to try to estimate the minimum dimensions required for our samples. Heat flow was assumed to be into a 'square' region, with thickness equal to radius. Three sets of program executions were made, varying the ratio of contact radius to outside radius from 0.001 to 1.0:

- 1) Gold: $k = 318 \text{ W/m}\cdot\text{K}$
 $Q = 1000 \text{ W}$
- 2) Gold: $k = 318 \text{ W/m}\cdot\text{K}$
 $Q = 100 \text{ W}$
- 3) Sapphire: $k = 35 \text{ W/m}\cdot\text{K}$
 $Q = 1000 \text{ W}$

The maximum contact temperature was achieved as the ratio of radii tends to zero. The contact temperature was normalized by dividing it by this maximum temperature. A plot of the normalized temperature as a function of the ratio of radii, shown in Figure 3.3, revealed that the normalized temperature is independent of both the materials thermal conductivity and the power input.

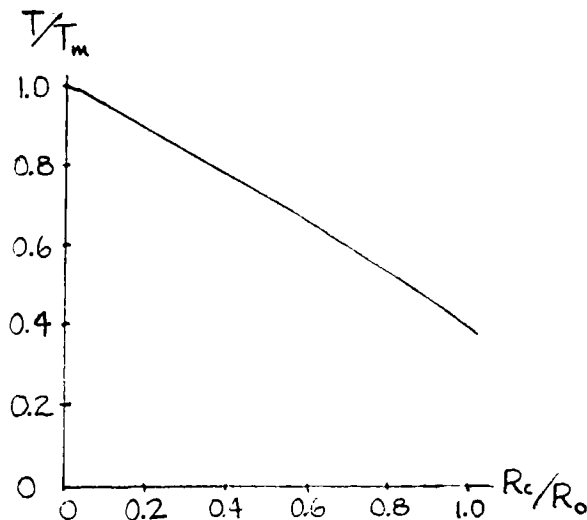


Figure 3.3
Temperature as a function of sample dimensions

Figure 3.3 indicates that to be within one percent of the maximum temperature attainable, the outside radius (and thickness) of the sample must be at least forty

times the contact radius. For our experimental apparatus, this corresponds to about seven millimeters.

It should be noted that this formulation considers heat flow into a finite medium, at equilibrium for a long period of time. In using the thermal comparator, steady heat flow into an effectively infinite medium is established, but a steady state temperature distribution throughout the sample is not established. We are probably safe using samples as much as thirty percent smaller than this, provided that the samples have a fairly high specific heat, and their temperature increase during testing is minimal.

3.2.3 Heat flux profile analysis

As mentioned at the end of Section 2.2.4, the thermal constriction resistance definitions used in the analytical modelling were derived assuming an isothermal contact spot, ie a temperature gradient over the surface of the form:

$$\frac{\partial T}{\partial z} (z=0) = - \frac{Q}{2\pi ka} \left[a^2 - r^2 \right]^{-\frac{1}{2}} \quad (1)$$

This assumption may introduce error in the film conductivity values found from the model, as the contact spot is almost certainly not isothermal.

The finite element model was used to gain a better understanding of the relationship between the assumed flux profile and the resulting thermal constriction resistance.

Two flux profiles were compared to the isothermal profile. The first, constant over the radius of the spot, was:

$$\frac{\partial T}{\partial z} (z = 0) = - \frac{Q}{\pi ka^2} \quad (2)$$

The second, which decreases with 'r', is:

$$\frac{\partial T}{\partial z} (z = 0) = - \frac{3Q}{2\pi k a^2} \left[1 - \left[\frac{r}{a} \right]^4 \right] \quad (3)$$

The three flux profiles, when integrated over the contact spot, all result in the same power input, 'Q'.

Finite element modelling yielded discrete temperature values for each node on the contact surface. The mean temperature over the surface was found using the relation:

$$\bar{T} = \frac{2}{a^2} \sum_{i=1}^n T_i r_i \Delta r$$

where 'a' is the radius of the contact spot, 'n' is the number of nodes, 'T' and 'r' are the temperature and radial location of the node, and Δr is the radial node spacing.

Using a contact radius of 0.25, an input power of 1000, a bulk material with a thermal conductivity of 50, and nine equally spaced nodes over the contact radius, the following results were obtained:

Profile	\bar{T}	$R = \frac{\bar{T}}{Q}$
(1)	15.314	0.015314
(2)	16.712	0.016712
(3)	17.700	0.017700

Table 3.1

Variation of the thermal constriction resistance with the heat flux profile

It can be seen that as the distribution of power shifts inward, the mean temperature of the contact surface increases. This increases the thermal constriction resistance about 15 percent.

Relating this change in the thermal constriction resistance to possible modelling error is not straightforward. The two resistance definitions equated (one with, the other without a film) assume the same profile. Although this profile is probably not accurate, the effects would tend to cancel.

3.3 Summary

The finite element model developed was useful for investigating various aspects of heat flow in a sample, including the estimation of minimum sample dimensions required for accurate results, and the effect of the assumed flux profile on the thermal constriction resistance.

Future modelling should include the probe tip. This may lead to a method of finding the thermal conductivity of a single film in a multilayer stack, and an estimate of the error associated with the analytical modelling.

4.0 CONCLUSION

Considerable progress has been made in using the thermal comparator to measure the thermal conductivity of thin solid films. The experimental apparatus has been improved and expanded to increase the accuracy of data and the speed of data collection. A two dimensional heat flow model was developed to extract the film thermal conductivity from the net film/substrate value read by the thermal comparator. Four dielectric thin film materials and two deposition techniques have been studied, and thermal finite element analysis has been performed.

Experimental work should continue in the future. A library of thin film thermal conductivities should be developed as a means of determining methods by which the thermal conductivity of optical coatings may be enhanced. The effect of the use of ion beam assist while depositing evaporated films should be examined. The thermal conductivity of films deposited by chemical vapor deposition should be examined.

At the present time, multilayer coatings can only be studied in an indirect manner. The nature of interfacial barriers can be investigated by depositing alternate layers of two or more coating materials. If the total number of films per sample is varied between samples, this could provide information concerning the insulative or conductive nature of the interfaces.

One area of particular interest is the study of highly conductive films such as diamond or metals. This could be accomplished using substrates of low thermal conductivity, such as silica. The 2-D heat flow model developed should be capable of extracting the thermal conductivity of highly conductive films as well as insulating films.

The nature of the physical contact and heat flow radius between the probe tip and specimen should be further investigated, by finite element analysis and infrared thermography. This could verify the heat flow radius used at the present, as well as provide information about the deformation of soft films. Development of a "correction factor" to estimate the contact temperature from the output millivoltage would enable the use finite element analysis in extracting the thermal conductivity of a single film from a multilayer stack.

A recent paper suggests that the thermal constriction resistance has been defined for the case of a film of variable thermal conductivity on the surface of a bulk material [23]. This may lead to a more accurate spatial description of the thermal conductivity of dielectric films, and should be investigated.

As a final note, it may be possible (although difficult) to numerically or analytically define the thermal constriction resistance for multiple coatings. If this can be accomplished, it would provide a direct, accurate means of determining the conductivity of a single film in a multilayer stack. Appendix V shows how the thermal constriction resistance could be defined for the case of multiple films on the surface of and infinite half-space.

REFERENCES

- [1] Proc 5th Conf. on Thermal Conductivity, Denver, CO (1965).
- [2] G. S. Mathad, P. W. Ing, C. Y. Ho and R. E. Taylor (eds.), Proc. 8th Conf. on Thermal Conductivity, Plenum Press, New York, p.713 (1969).
- [3] P. Nath and K. L. Chopra, "Experimental Determination of the Thermal Conductivity of Thin Films," Thin Solid Films, **18**, pp.29-37 (1973)
- [4] V. M. Abrosimov, Soviet Phys. Solid State, **11**, p.2 (1969)
- [5] B. S. Fraiman and A. F. Chudnovski, Fiz. Tekh. Polyprov., USSR, **5**, pp.242-6, (1971). (English translation in Soviet Phys. Semiconductors, USA).
- [6] F. Kelemen, "Pulse Method for the Measurement of the Thermal Conductivity of Thin Films," Thin Solid Films, **36**, pp.199-203 (1976).
- [7] D. L. Decker, L. G. Koshigoe, and E. J. Ashley, "Thermal Properties of Optical Thin Film Materials," Laser Induced Damage in Optical Materials: 1984, NBS Special Publication 727, pp. 291-7 (1986).
- [8] D. Ristau and J. Ebert, "Development of a Thermographic Laser Calorimeter," Appl. Optics, **25**, pp.4571-8 (1986).
- [9] R. W. Powell, "Experiments using a simple thermal comparator for measurement of thermal conductivity, surface roughness, and thickness of foils or of surface deposits," J. Sci. Instrum., **34**, pp.485-92 (1957).
- [10] R. W. Powell, H. Groot, and D. P. DeWitt, "Thermal Comparator Developments," in Proc. 8th Conf. on Thermal Conductivity, G. S. Mathad, P. W. Ing, C. Y. Ho and R. E. Taylor (eds.), Plenum Press, New York, pp.771-9 (1969).

- [11] R. W. Powell, "Thermal Conductivity Determinations by Thermal Comparator Methods," Chapter 6 in Thermal Conductivity, R. P. Tye (ed.), Academic Press, London, pp.275-338 (1969).
- [12] S. Timoshenko and J. N. Goodier, "Pressure between Two Spherical Bodies in Contact," Section 125 in Theory of Elasticity, McGraw-Hill Book Co., New York, pp. 372-77 (1951).
- [13] TC-1000 Thermal Comparator, Lafayette Instrument Company, Lafayette, IN.
- [14] D. C. Ginnings, "Powell-Comparator Method for Determining Thermal Conductivities - A Discussion," in Progress in International Research on Thermodynamic and Transport Properties, J. F. Masi and D. H. Tsai (eds.), Academic Press, New York, pp.474-80 (1962).
- [15] W. T. Clark and R. W. Powell, "Measurement of thermal conduction by the thermal comparator," J. Sci. Instrum., 39, pp.545-51 (1962).
- [16] H. S. Carslaw and J. C. Jaeger, "The flow of heat in regions bounded by surfaces of the cylindrical coordinate system," Chapter VIII in Conduction of Heat in Solids, Oxford University Press, London, p.216 (1959).
- [17] J. R. Dryden, "The Effect of a Surface Coating on the Constriction Resistance of a Spot on an Infinite Half-Plane," J. Heat. Trans., 105, pp.408-10 (1983).
- [18] M. L. Scott, H.E. Bennett, A. H. Guenther, D. Milam, and B. E. Newman, "A Review of UV Coating Materials Properties," Symp. on Optical Materials for High Power Lasers (Boulder, CO, 1983), pp.329-39.
- [19] S. S. Ballard and J. S. Browder, "Thermal Properties," Section 1.1.1.3 of CRC Handbook of Laser Science and Technology, Vol. IV, Part 2, (ed) M. J. Weber, CRC Press, Boca Raton, FL (1986).
- [20] Y. S. Touloukian, R. W. Powell, C. Y. Ho, P. G. Klemens, Thermophysical Properties of Matter, Volume 2, Thermal Conductivity, Non-Metallic Solids, IFI/Plenum Data Corporation, New York, p.208 (1970).

- [21] W. A. Hargreaves, "Tech Note: Magnesium Fluoride-Update and Summary of Optical Properties," Laser Focus, 18, p.86 (1982).
- [22] J. N. Reddy, An Introduction to the Finite Element Method, McGraw-Hill Book Co., New York, pp.206-210 (1984).
- [23] K. J. Negus, C. A. Vanoverbeke, and M. M. Yovanovich, "Thermal Constriction Resistance with Variable Thermal Conductivity Near the Contact Surface," included in Fundamentals of Conduction and Recent Developments in Contact Resistance, M. Imber, G. P. Peterson, and M. M. Yovanovich (Eds.), ASME Special Publication HTD-Vol 69 (1987).
- [24] A. Redondo, and J. G. Beery, "Thermal conductivity of optical coatings," J. Appl. Phys, 60, pp.3882-5 (1986).
- [25] S. D. Jacobs, S. E. Gilman, D. J. Smith, D. G. Angeley, and J. C. Lambropoulos, "Thermal Conductivities for Thin films of SiO₂, Al₂O₃, and MgF₂ on Dielectric Substrates," LLE Review, 29, Laboratory for Laser Energetics, University of Rochester, Rochester, NY (1987).
- [26] M. L. Jones, G. M. Smith, and J. C. Wolford, "Curvefitting," Chapter 4 in Applied Numerical Methods for Digital Computation, Harper and Row, Publishers, New York (1985).
- [27] I. N. Sneddon, "Axisymmetric Dirichlet problem for a half-space," Section 5-10-1 of The Use of Integral Transforms, McGraw-Hill Book Co., New York, pp.325-6 (1972).

ACKNOWLEDGEMENT

This work should be viewed as one part of a long term investigation under the supervision of Dr. Jacobs at the Laboratory for Laser Energetics, University of Rochester. Work began in 1984, long before I started. I hope that funding will continue to be available for work to continue in the future, as this technique may eventually lead to optical coatings capable of withstanding much higher thermal loads.

I had considerable help with the experimental aspects of this project, particularly from Scott Gilman, an Optics student at the University of Rochester. He helped me with data collection, programming of the personal computer used in data acquisition, and with the optical measurement of the probe tip.

This work was supported in part by Optical Coating Laboratory, Inc. of Santa Rosa, CA; the New York State Center for Advanced Optical Technology of the Institute of Optics; the U. S. Department of Energy Office of Inertial Fusion Research under agreement No. DE-FC08-85DP40200; and by the Laser Fusion Feasibility Project at the Laboratory for Laser Energetics which has the following sponsors: Empire State Electric Energy Research Corporation, New York State Energy Research and Development Authority, Ontario Hydro, and the University of Rochester. Such support does not imply endorsement of the content by the above parties.

APPENDIX I - CURVEFITTING

This cubic spline curvefitting program package was written to fit a curve to data taken from standards with the thermal comparator apparatus. A cubic polynomial is fit between each pair of data points, matching first and second derivatives between each curve. The exponential of the input thermal conductivities are considered to be a function of the input millivoltages.

The endpoints of the outer splines are considered free, ie locations of zero second derivative. Cubic spline fits, in general, require that all the data points to be fit fall between points used to generate the curves.

A total of four subroutines are called by the main program CFIT. CUBIC is the routine which calculates the derivative data for each spline, using the simultaneous equation solver GAUSS, and its accompanying routine SCPIVOT. Once the spline data is generated, the subroutine INTERP fits data from the specimens of unknown thermal conductivity to the curves. The subroutines GAUSS and SCPIVOT are also used in finite element analysis, and appear in Appendix IV.

Two sets of data are read by CFIT: the number of points to fit curves to, followed by the data points themselves, and the number of unknown data points, followed by their millivoltage values.

```

*****
*
*   PROGRAM           :           CFIT
*
*   PROGRAMMER       :           C. AMSDEN
*
*   DATE WRITTEN    :           7 - 87
*
*   OBJECTIVE:
*       THE PURPOSE OF THIS PROGRAM IS TO FIT A CUBIC 'NATURAL
*       SPLINE' POLYNOMIAL TO A SET OF INPUT DATA, AND EVALUATE
*       THE RESULTING FUNCTION AT DESIRED POINTS ENCLOSED IN THE
*       DATA DOMAIN. AS THE TERM 'NATURAL SPLINE' INDICATES,
*       THE ENDPOINTS ARE CONSIDERED FREE, IE INFLECTION POINTS.
*       LOGARITHMIC SCALING IS PERFORMED TO INCREASE ACCURACY.
*       THEREFORE, ALL INPUT Y VALUES MUST BE GREATER THAN ZERO.
*
*   SUBPROGRAMS REFERENCED:
*       CUBIC(MAXM,M,X,Y,H,A,B,ICOL,YDP)
*           SUBROUTINE WHICH PERFORMS THE CUBIC POLYNOMIAL
*           APPROXIMATION. IT RETURNS THE SECOND DERIVATIVE
*           VALUES AT THE INTERIOR NODES, WHICH ARE USED TO
*           EVALUATE THE FUNCTION.
*       GAUSS(MAXN,N,A,B,X,ICOL,SUCCESS)
*           SUBROUTINE TO PERFORM GAUSSIAN ELIMINATION.
*           CALLED THROUGH CUBIC.
*       SCPIVOT(MAXN,N,A,B,X,ICOL,SUCCESS)
*           SUBROUTINE TO SCALE AND COLUMN PIVOT AN
*           AUGMENTED MATRIX. CALLED THROUGH GAUSS.
*       INTERP(MAXM,M,MAXNF,NF,X,Y,YDP,Z,FZ)
*           SUBROUTINE TO EVALUATE THE CUBIC POLYNOMIAL
*           APPROXIMATION AT DESIRED LOCATIONS.
*
*   ARRAYS USED:
*       X           :           X VALUES, INPUT DATA TO FIT CURVE TO
*       Y           :           Y VALUES, INPUT DATA TO FIT CURVE TO
*       YDP         :           SECOND DERIVATIVE VALUES AT INTERIOR
*                               NODES (DATA POINTS)
*       A           :           COEFFICIENT MATRIX USED BY CUBIC
*       B           :           RESIDUAL VECTOR USED BY CUBIC
*       H           :           DIFFERENCE IN X VALUES OF NEIGHBORING
*                               NODES (DATA POINTS)
*       Z           :           X VALUES WHOSE FUNCTION VALUE IS SOUGHT
*       FZ          :           FUNCTION VALUE SOUGHT
*
*   VARIABLES USED:
*       MAXM        :           PARAMETER - MAX NUMBER OF DATA POINTS
*       MAXNF       :           PARAMETER - MAX NUMBER OF FUNCTION VALUES
*                               SOUGHT
*       M           :           ACTUAL NUMBER OF DATA VALUES USED
*       NF          :           ACTUAL NUMBER OF FUNCTION VALUES SOUGHT
*
*****
*
*   PROGRAM CFIT
*
*   INTEGER*4 MAXM,MAXNF
*   PARAMETER (MAXM=50,MAXNF=50)
*   INTEGER*4 M,NF,ICOL(MAXM-2)
*   REAL*4 X(MAXM),Y(MAXM),YDP(MAXM),A(MAXM-2,MAXM-2),B(MAXM-2),

```



```

+          H(MAXM-2),Z(MAXNF),FZ(MAXNF)
*
*   READ(5,*)M
*
*   DO 100 I=1,M
*       READ(5,*) X(I),Y(I)
*       IF (Y(I).LE.0.0) THEN
*           WRITE(6,*) 'INPUT NON-POSITIVE Y VALUE'
*           STOP
*       ENDIF
*       Y(I)=LOG(Y(I))
100  CONTINUE
*
*   CALL CUBIC(MAXM,M,X,Y,H,A,B,ICOL,YDP)
*
*   READ(5,*) NF
*
*   DO 200 I=1,NF
*       READ(5,*) Z(I)
200  CONTINUE
*
*   CALL INTERP(MAXM,M,MAXNF,NF,X,Y,YDP,Z,FZ)
*
*   WRITE(6,5)
5    FORMAT('0',11X,'V',16X,'KAPP',/,5X,<31>('-'))
*
*   DO 300 I=1,NF
*       FZ(I)=EXP(FZ(I))
*       WRITE(6,15) Z(I),FZ(I)
15   FORMAT('0',5X,E13.7,5X,E13.7)
300  CONTINUE
*
*   STOP
*   END

```

```

*****
*
*      SUBROUTINE      :      CUBIC
*
*      PROGRAMMER     :      C. AMSDEN
*
*      DATE WRITTEN   :      7 - 87
*
*      OBJECTIVE:
*      GIVEN A SET OF INPUT DATA POINTS, THIS SUBROUTINE WILL
*      DO A CUBIC 'NATURAL SPLINE' POLYNOMIAL APPROXIMATION OVER
*      EACH INTERVAL BETWEEN DATA POINTS. THIS SUBROUTINE RETURNS
*      A SECOND DERIVATIVE VALUE FOR EACH INTERIOR POINT. AS THE
*      TERM 'NATURAL SPLINE' IMPLIES, THE ENDPOINTS OF THE RANGE
*      ARE ASSUMED INFLECTION POINTS.
*
*      SUBPROGRAMS REFERENCED:
*      GAUSS(MAXN,N,A,B,X,SUCCESS,ICOL)
*      SUBROUTINE TO PERFORM GAUSSIAN ELIMINATION
*      SCPIVOT(MAXN,N,A,B,K,ICOL,SUCCESS)
*      SUBROUTINE TO SCALE AND COLUMN PIVOT AN AUGMENTED
*      MATRIX BEFORE GAUSSIAN ELIMINATION IS PERFORMED.
*      CALLED THROUGH GAUSS
*
*      ARRAYS USED:
*      X      :      INPUT X VALUES OF DATA POINTS
*      Y      :      INPUT Y VALUES OF DATA POINTS
*      H      :      DIFFERENCE IN ADJACENT X VALUES
*      A      :      COEFFIEIENT MATRIX
*      B      :      RESIDUAL MATRIX
*      YDP    :      SECOND DERIVATIVE VALUES SOUGHT
*      ICOL   :      REORDER MATRIX USED BY GAUSS
*
*      VARIABLES USED:
*      MAXM   :      PARAMETER - MAX NUMBER OF INPUT
*                  DATA POINTS
*      M      :      ACTUAL NUMBER OF DATA POINTS
*      N      :      NUMBER OF SPLINES (N=M-1)
*      SUCCESS :      LOGICAL VARIABLE - GAUSS SUCCESSFUL
*
*****
*
*      SUBROUTINE CUBIC(MAXM,M,X,Y,H,A,B,ICOL,YDP)
*
*      INTEGER*4 MAXM,M,N,ICOL(MAXM-2)
*      REAL*4 X(MAXM),Y(MAXM),H(MAXM-1),A(MAXM-2,MAXM-2),
+      B(MAXM-2),YDP(MAXM-2)
*      LOGICAL*1 SUCCESS
*
*      N=M-1
*
*      DO 100 I=1,N
*          H(I)=X(I+1)-X(I)          !DETERMINE H VALUES
100  CONTINUE
*
*      A(1,1)=2.0*(H(1)+H(2))
*      A(1,2)=H(2)                  !FILL COEFFIEIENT MATRIX
*
*      DO 200 I=2,N-2
*          A(I,I-1)=H(I)

```

```

                A(I,I)=2.0*(H(I)+H(I+1))
                A(I,I+1)=H(I+1)
200      CONTINUE
*
      A(N-1,N-2)=H(N-1)
      A(N-1,N-1)=2.0*(H(N-1)+H(N))
*
                                !FILL RESIDUAL VECTOR
      DO 300 I=1,N-1
      B(I)=6.0*((Y(I+2)-Y(I+1))/H(I+1)-(Y(I+1)-Y(I))/H(I))
300      CONTINUE
*
      CALL GAUSS(MAXM-2,M-2,A,B,YDP,SUCCESS,ICOL)
      IF (.NOT.SUCCESS) THEN
+        WRITE(6,*) 'GAUSS ELIMINATION FAILED DUE TO ',
          'DIVISION BY ZERO, PROGRAM ABORTED.'
          STOP
*        ENDIF
      RETURN
      END

```

```

*****
*
*      SUBROUTINE      :      INTERP
*
*      PROGRAMMER     :      C. AMSDEN
*
*      DATE WRITTEN   :      7 - 87
*
*      OBJECTIVE:
*      THE PURPOSE OF THIS SUBROUTINE IS TO SUPPLY FUNCTION
*      VALUES FOR CORRESPONDING INPUT DATA.  THE FUNCTION USED
*      IS A CUBIC 'NATURAL SPLINE' POLYNOMIAL APPROXIMATION
*      MADE TO A SET OF DATA POINTS BY THE SUBROUTINE CUBIC.
*      THE DRIVER PROGRAM SUPPLIES THE SECOND DERIVATIVE VALUES,
*      FOUND BY CUBIC, WHICH THIS SUBROUTINE USES TO FIND THE
*      DESIRED FUNCTION VALUES.  IT SHOULD BE NOTED THAT THE
*      SECOND DERIVATIVE VALUES ARE DISTINGUISHED BY INTERIOR
*      NODE INDICES, AND THAT CORRECTION IS MADE IN THIS
*      SUBROUTINE TO INCLUDE THE TWO RANGE ENDPOINTS.
*
*      ARRAYS USED:
*      X      :      X VALUES CURVE FIT TO
*      Y      :      Y VALUES CURVE FIT TO
*      YDP    :      SECOND DERIVATIVE OF FUNCTION AT NODES
*      Z      :      X VALUE WHOSE Y VALUE IS SOUGHT
*      FZ     :      FUNCTION EVALUATED AT X
*
*      VARIABLES USED:
*      MAXM   :      PARAMETER - MAX NUMBER OF DATA POINTS USED
*                  IN FITTING CURVE
*      MAXNF  :      PARAMETER - MAX NUMBER OF FUNCTION
*                  VALUES SOUGHT
*      M      :      ACTUAL NUMBER OF DATA POINTS USED
*      NF     :      ACTUAL NUMBER OF FUNCTION VALUES SOUGHT
*      I      :      INTERVAL, OR SPLINE INDEX
*      J      :      COUNTER
*      S      :      SPLINE CONTAINING Z VALUE
*      H      :      WORKING VARIABLE - DIFFERENCE IN X VALUES
*                  AT SPLINE ENDPOINTS
*      D1     :      WORKING VARIABLE - DIFFERENCE BETWEEN Z AND
*                  SMALL SPLINE X VALUE
*      D2     :      WORKING VARIABLE - DIFFERENCE BETWEEN LARGE
*                  SPLINE X VALUE AND Z
*
*****
*
*      SUBROUTINE INTERP(MAXM,M,MAXNF,NF,X,Y,YDP,Z,FZ)
*
*      INTEGER*4 MAXM,MAXNF,M,NF,I,J,S
*      REAL*4 X(MAXM),Y(MAXM),YDP(MAXM),Z(MAXNF),FZ(MAXNF),H,DI,D2
*
*      YDP(M)=0.0
*      DO 100 J=M-1,2,-1          !CORRECT SECOND DERIVATIVE
*          YDP(J)=YDP(J-1)      !INDICES TO INCLUDE ENDPOINTS
100  CONTINUE
*      YDP(1)=0.0
*
*      DO 200 J=1,NF
*          S=0
*          DO 400 I=1,M-1
*              !FIND INTERVAL Z CONTAINED IN

```

```

400      IF ((Z(J).GE.X(I)).AND.(Z(J).LE.X(I+1))) S=I
*      CONTINUE
      IF (S.EQ.0) THEN
        WRITE(6,5) Z(J)
5        FORMAT(' ',5X,E13.7,2X,'OUT OF RANGE')
      ELSE
        H=X(S+1)-X(S)
        D1=X(S+1)-Z(J)          !FIND FZ
        D2=Z(J)-X(S)
        FZ(J)=(YDP(S)/6.0)*(D1**3/H-H*D1)
+         +(YDP(S+1)/6.0)*(D2**3/H-H*D2)
+         +Y(S)*D1/H+Y(S+1)*D2/H
      ENDIF
200     CONTINUE
*     RETURN
      END

```

APPENDIX II - ROOTFINDING

This rootfinding program package was written to find the zero intercept of the function generated by equating two definitions of the thermal constriction resistance. The zero intercept corresponds to the thin film thermal conductivity.

Two subprograms are used by the main program GETK1: BISECT, which finds the root of the input function, and F, the function whose root is sought.

The subroutine BISECT was modified specifically for use with monotonically decreasing functions. If the solution is not found within the initial estimated range, the program searches orders of magnitude in the correct direction until the solution is found, or search the criterion is exceeded.

Nine parameters are input into the program. The first three are used in evaluating the function: the ratio of film thickness to contact radius, the substrate conductivity, and the apparent conductivity. The fourth refers to the maximum number of summations to be performed in evaluating the function, the fifth to summation convergence criterion (the ratio of last to first terms). The sixth term is the relative convergence criteria used by BISECT to determine if the solution has been found to the desired accuracy. The seventh and eighth are the lower and upper bounds of the range to be searched, which should span one order of magnitude, and the ninth is the maximum number of orders of magnitude to search.

Figure II.1 shows the general form of the function. Table II.1 shows the results of program execution for a variety of film thickness to heat flow radius ratios, and apparent to substrate conductivity ratios.

It should be noted that forward summation (large to small) of a slowly converging series can potentially result in computer roundoff error. Later terms, being orders of magnitude smaller than the initial ones, are dropped. The effect of several thousand small terms, however, may significantly alter the solution. Forward and reverse (small to large) summation techniques were compared for this function, and found to be virtually identical.

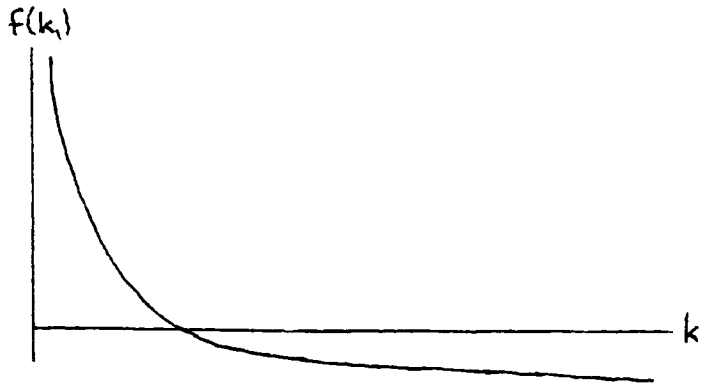


Figure II.1
2-D model function

k_1 values, taken for $k_2 = 150.0$

k_{app}/k_2	t/a				
	0.001	0.01	0.1	1.0	10.0
5.0	1168100	116830	11733	1518.3	805.25
1.0	150.0	150.0	150.0	150.0	150.0
0.95	3.5691	32.568	113.77	139.68	142.26
0.90	1.6921	16.112	86.904	129.64	134.55
0.70	0.43743	4.2443	34.343	92.457	103.89
0.50	0.18569	1.8221	15.772	60.122	73.599
0.30	0.079613	0.78121	6.9118	32.649	43.750
0.10	0.02047	0.20261	1.8098	9.8121	14.427
0.05	0.0091476	0.095863	0.85866	4.7791	7.1922
0.01	0.0018796	0.018068	0.16498	0.93583	1.4352
0.005	-	0.0090782	0.081980	0.46670	0.71741

Table II.1
Film conductivity as a function of
normalized film thickness and conductivity

```

*****
*
*   PROGRAM           :   GETK1
*
*   PROGRAMMER       :   C. AMSDEN
*
*   DATE WRITTEN    :   7 - 87
*
*   OBJECTIVE:
*       THE PURPOSE OF THIS PROGRAM IS TO FIND THE THERMAL
*       CONDUCTIVITY OF A THIN FILM. THIS IS ACCOMPLISHED
*       BY IMPLEMENTING THE MODIFIED BISECTION METHOD, AND
*       SOLVING THE 2-D HEAT FLOW EQUATION.
*
*   NOTE:
*       THE BISECTION ROUTINE USED HAS BEEN MODIFIED SO THAT
*       IF THERE IS ZERO OR AN EVEN NUMBER OF ROOTS IN THE
*       GIVEN RANGE, THE RANGE CAN BE MODIFIED AND THE METHOD
*       RE-EXECUTED. FOR THIS REASON, K1MIN AND K1MAX DO NOT
*       NECESSARILY HAVE TO ENCLOSE THE ROOT. THIS PROGRAM
*       WILL MODIFY THE RANGE AN ORDER OF MAGNITUDE IN THE
*       CORRECT DIRECTION UNTIL THE ROOT IS ENCLOSED. THIS
*       PROGRAM WILL ONLY WORK FOR MONOTONICALLY DECREASING
*       FUNCTIONS.
*
*   SUBPROGRAMS REFERENCED:
*       BISECT(F,K1MIN,K1MAX,EPSR,CONV,COND1,COND2,K1,IT)
*           MODIFIED BISECTION SUBROUTINE TO FIND K1
*       F(K1)   FUNCTION TO BE SOLVED.
*
*   VARIABLES USED:
*       TR      :   RATIO OF FILM THICKNESS TO PROBE
*                   CONTACT RADIUS
*       K1      :   FILM CONDUCTIVITY
*       K2      :   SUBSTRATE CONDUCTIVITY
*       KAPP    :   APPARENT CONDUCTIVITY - AS MEASURED
*                   BY THE THERMAL COMPARATOR
*       VR      :   RATIO OF LAST TO FIRST TERM SUMMED
*                   IN FUNCTION (TELLS WHEN TO STOP SUMMING)
*       K1MIN   :   LOW INITIAL GUESS
*       K1MAX   :   HIGH INITIAL GUESS
*       EPSR    :   RELATIVE ERROR IN SOLUTION - NEGATIVE
*                   EXPONENT VALUE IS NUMBER OF SIGNIFICANT
*                   DIGITS IN SOLUTION.
*       N       :   MAXIMUM NUMBER OF SUMMATIONS FOR FUNCTION
*                   TO PERFORM
*       J       :   SUMMATIONS ACTUALLY PERFORMED
*       IT      :   ITERATIONS PERFORMED BY BISECT
*       ORDERS  :   NUMBER OF ORDERS OF MAGNITUDE SEARCHED
*       MAXORD  :   MAXIMUM NUMBER OF ORDERS TO SEARCH
*       CONV    :   LOGICAL VARIABLE - METHOD CONVERGED
*       COND1   :   LOGICAL VARIABLE - SEARCH RANGE LOW
*       COND2   :   LOGICAL VARIABLE - SEARCH RANGE HIGH
*
*****
*
*   PROGRAM GETK1
*
*   REAL*4 TR,K1,K2,KAPP,VR,F,K1MIN,K1MAX,EPSR
*   INTEGER*4 N,J,IT,ORDERS,MAXORD
*   LOGICAL*1 CONV,COND1,COND2

```



```

*
COMMON TR,K2,KAPP,N,J,VR
EXTERNAL F
*
READ(5,*) TR,K2,KAPP,N,VR,EPSR,K1MIN,K1MAX,MAXORD
*
ORDERS=0
*
DO 100 WHILE (ORDERS.LT.MAXORD)           !SEARCH VARIOUS ORDERS
ORDERS=ORDERS+1                           !OF MAGNITUDE
*
CALL BISECT(F,K1MIN,K1MAX,EPSR,CONV,COND1,COND2,K1,IT)
*
IF (CONV) THEN
WRITE(6,5) K1,ORDERS,IT,J
5   FORMAT('0',5X,'THE SOLUTION IS K1 = ',E10.5,/,7X,
+     'THE SOLUTION WAS FOUND AFTER SEARCHING',I2,/
+     7X,'ORDER(S) OF MAGNITUDE, WITH ',I2,' ITERATION
+     /,7X,'OF THE BISECTION METHOD. THE LAST TERM',
+     /,7X'INCLUDED',I6,' SUMMATIONS.',/)
STOP
ELSEIF (COND1) THEN                       !RANGE LOW,
K1MIN=K1MAX                               !INCREASE IT
K1MAX=10.0*K1MAX                         !ONE ORDER
ELSE
K1MAX=K1MIN                               !RANGE HIGH,
K1MIN=0.1*K1MIN                          !DECREASE IT
ENDIF                                     !ONE ORDER
*
100 CONTINUE
*
WRITE(6,15) ORDERS
15  FORMAT('0',5X,I2,' ORDER(S) OF MAGNITUDE SEARCHED, THE',
+     ' SOLUTION WAS NOT FOUND.',/)
*
STOP
END

```

```

*****
*
*      SUBROUTINE      :      BISECT
*
*      PROGRAMMER     :      C. AMSDEN
*
*      DATE WRITTEN   :      7 - 87
*
*      OBJECTIVE:
*      THE PURPOSE OF THIS SUBROUTINE IS TO DETERMINE WHETHER
*      THERE IS A ROOT ENCLOSED IN A SPECIFIED RANGE, AND IF
*      SO FIND IT. AN EVEN NUMBER OF ROOTS APPEARS THE SAME
*      AS NO ROOTS. IF IT APPEARS NO ROOTS ARE ENCLOSED, THIS
*      SUBROUTINE RETURNS INFORMATION THAT MAY BE USED BY THE
*      DRIVER PROGRAM TO MODIFY THE RANGE. ONCE IT APPEARS
*      A ROOT IS ENCLOSED, THE RANGE IS BISECTED UNTIL THE
*      ERROR CRITERION IS MET.
*
*      SUBPROGRAMS REFERENCED:
*      F(X)      FUNCTION WHOSE ROOT IS SOUGHT
*
*      VARIABLES USED:
*      X1      :      LOW END OF RANGE
*      X2      :      HIGH END OF RANGE
*      XMID    :      MIDPOINT OF RANGE
*      F1      :      F(X1)
*      F2      :      F(X2)
*      FMID    :      F(XMID)
*      EPSR    :      RELATIVE ERROR CRITERION - THE
*                       VALUE OF THE NEGATIVE EXPONENT
*                       IS EQUAL TO THE NUMBER OF SIGNIFICANT
*                       DIGITS IN THE SOLUTION.
*      ERROR   :      ERROR IN PRESENT SOLUTION
*      IT      :      ITERATIONS (BISECTIONS) PERFORMED
*      CONV    :      LOGICAL VARIABLE - METHOD CONVERGED
*      COND1   :      LOGICAL VARIABLE - BOTH FUNCTION VALUES
*                       POSITIVE
*      COND2   :      LOGICAL VARIABLE - BOTH FUNCTION VALUES
*                       NEGATIVE
*
*****
*
*      SUBROUTINE BISECT(F,X1,X2,EPSR,CONV,COND1,COND2,X,IT)
*
*      REAL*4 X,X1,X2,XMID,F,F1,F2,FMID,EPSR,ERROR
*      INTEGER*4 IT
*      LOGICAL*1 CONV,COND1,COND2
*
*      EXTERNAL F
*
*      IT=0
*      CONV=.FALSE.           !INITIALIZE
*      COND1=.FALSE.         !PARAMETERS
*      COND2=.FALSE.
*
*      F1=F(X1)               !INITIALIZE
*      F2=F(X2)               !FUNCTION VALUES
*
*      IF (F1.EQ.0.0) THEN
*          X=X1

```

```

        CONV=.TRUE.
        RETURN
    ELSEIF (F2.EQ.0.0) THEN
        X=X2
        CONV=.TRUE.
        RETURN
    ELSEIF ((F1.GT.0.0).AND.(F2.GT.0.0)) THEN
        COND1=.TRUE.
        RETURN
    ELSEIF ((F1.LT.0.0).AND.(F2.LT.0.0)) THEN
        COND2=.TRUE.
        RETURN
    ELSE
        ERROR=(X2-X1)/(X2+X1)
    ENDIF
*
    DO 100 WHILE (ABS(ERROR).GT.ABS(EPSR))
        IT=IT+1
*
        XMID=(X1+X2)/2.0
        FMID=F(XMID)
        IF (FMID.EQ.0.0) THEN
            X=XMID
            CONV=.TRUE.
            RETURN
        ELSEIF ((F1*FMID).LT.0.0) THEN
            X2=XMID
            F2=FMID
        ELSE
            X1=XMID
            F1=FMID
        ENDIF
*
        ERROR=(X2-X1)/(X2+X1)
100 CONTINUE
*
        X=(X1+X2)/2.0
        CONV=.TRUE.
*
        RETURN
    END

```

```

*****
*
*   FUNCTION           :           F
*
*   PROGRAMMER        :           C. AMSDEN
*
*   DATE WRITTEN     :           6 - 87
*
*   OBJECTIVE/BACKGROUND:
*       THE PURPOSE OF THIS FUNCTION IS TO SUPPLY VALUES OF THE
*       2-D THERMAL COMPARATOR HEAT FLOW EQUATION (ONE FILM), FOR
*       A GIVEN FILM CONDUCTIVITY. THIS FUNCTION IS INTENDED TO BE
*       USED WITH (ZERO) ROOT FINDING METHODS. THE EQUATION WAS
*       DERIVED BY METHODS OF OPERATIONAL CALCULUS.
*
*   VARIABLES USED:
*       K1           :           FILM CONDUCTIVITY
*       K2           :           SUBSTRATE CONDUCTIVITY
*       KAPP         :           APPARENT CONDUCTIVITY
*       TR           :           RATIO OF FILM THICKNESS TO PROBE CONTACT
*                               RADIUS.
*       V            :           TRANSIENT VALUE TO BE SUMMED
*       V1           :           FIRST VALUE SUMMED
*       VR           :           RATIO OF FINAL TO FIRST VALUE SUMMED
*                               ( TELLS WHEN TO STOP SUMMING )
*       N            :           MAXIMUM NUMBER OF SUMS TO BE PERFORMED
*       J            :           ACTUAL NUMBER OF SUMS PERFORMED
*       AJ           :           WORKING VARIABLE - ALPHA J
*       D            :           "           "
*       I            :           "           " - INTEGRAL
*       TH           :           "           " - THETA
*
*****
*
*   REAL*4 FUNCTION F(K1)
*
*   INTEGER*4 J,N
*   REAL*4 K1,K2,KAPP,TR,V,V1,VR,AJ,D,I,TH
*
*   COMMON TR,K2,KAPP,N,J,VR
*
*   J=0
*   S=0.0
*   V=0.0
*   V1=0.0
*   TH=(K1-K2)/(K1+K2)
*
*   DO 100 WHILE (ABS(V).GE.ABS(V1*VR))
*       J=J+1
*       AJ=2.0*TR*J
*       D=AJ/2.0+SQRT(.25*AJ**2+1.0)
*       I=-AJ+(D-1.0/(2.0*D))*SQRT(1.0-(1.0/(D**2)))
*       + .5*ASIN(1.0/D)
*       V=(TH**J)*I
*
*       IF (J.EQ.1) V1=V
*       S=S+V
*
*       IF (J.GT.N) THEN
*           WRITE(6,*) 'FUNCTION SUMMATION CRITERION EXCEEDED.'

```

```
                STOP
            ENDIF
100    CONTINUE
*
*      F=1.0/(4.0*K1)+2.0*S/(3.14159*K1)-1.0/(4.0*KAPP)
*
RETURN
END
```

APPENDIX III - CONTACT STRESS ANALYSIS

Problem Formulation

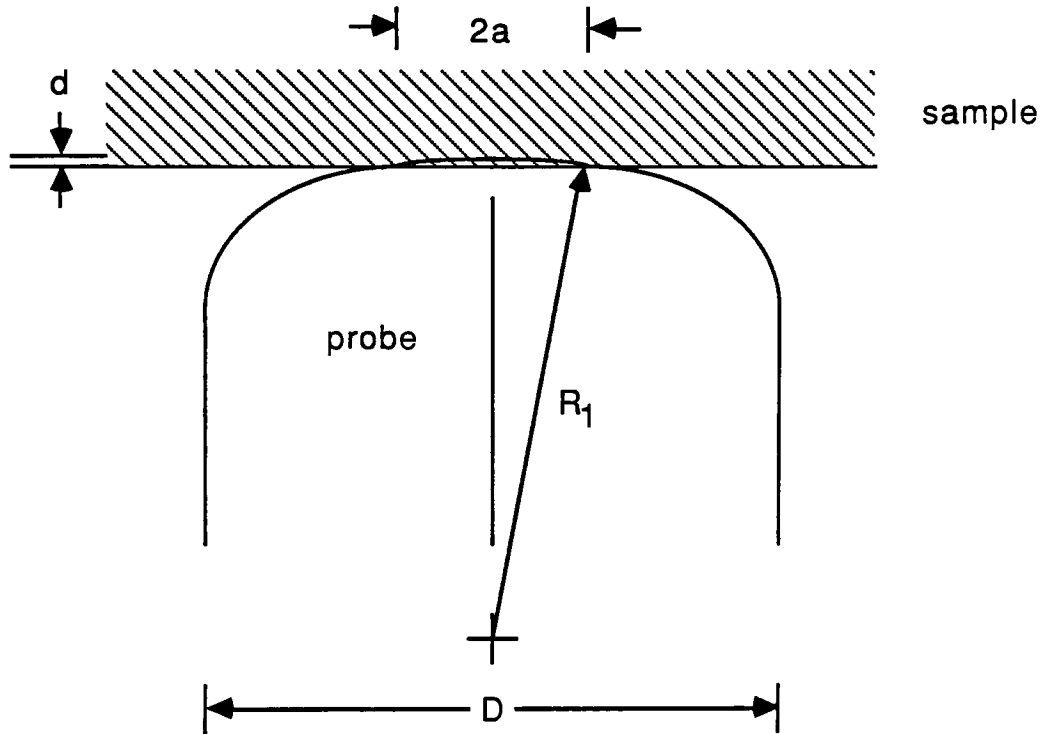


Figure III.1
Contact stress local geometry

Estimate:

- 1) The contact radius 'a'
- 2) The indentation made into the sample 'd'

Assumptions:

- 1) All deformation elastic
- 2) Probe tip made of pure constantan
- 3) $R_1 = D = 670$ microns (measured with an optical comparator)
- 4) Homogeneous materials

Governing Equations [12], for two spheres in contact:

$$a = \left[\frac{3\pi}{4} \frac{P(K_1 + K_2)R_1 R_2}{R_1 + R_2} \right]^{\frac{1}{3}}$$

$$d = \left[\frac{9\pi^2}{16} \frac{P^2 (K_1 + K_2)^2 (R_1 + R_2)}{R_1 R_2} \right]^{\frac{1}{3}}$$

where:

$$K_i = \frac{1 - \nu_i^2}{\pi E_i} \quad , i = 1, 2$$

P : compressive force

E : elastic modulus

ν : Poisson's ratio

R : radius

subscript definition:

1 : probe

2 : sample

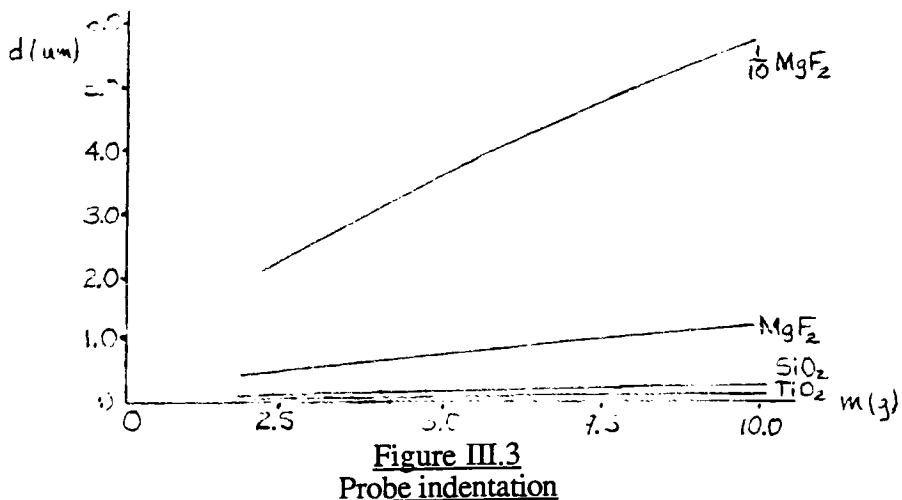
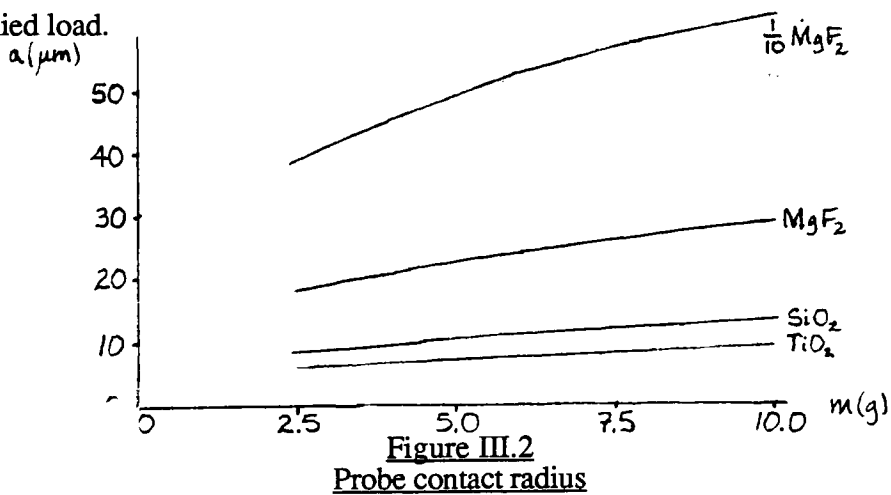
As the substrate is flat, it has an infinite radius. The governing equations become:

$$a = \left[\frac{3\pi}{4} P (K_1 + K_2) R_1 \right]^{\frac{1}{3}}$$

$$d = \left[\frac{9\pi^2}{16} \frac{P^2}{R_1} (K_1 + K_2)^2 \right]^{\frac{1}{3}}$$

The contact radii and probe penetrations were calculated assuming the modulus of elasticity and Poisson's ratio of constantan are 165.48 GPa and 0.25, respectively, and the Poisson's ratio of dielectric materials is 0.25. Film data was taken from Scott [18]. As there is considerable uncertainty involved with thin film properties, a 'worst case' calculations were made for a material ten times as soft as the softest film, Magnesium Fluoride. It should be noted that these calculations consider contact with a bulk material with thin film properties, not a film on substrate combination. In reality, the presense of a rigid substrate beneath the film will reduce deformation.

Figures III.2 and III.3 show the contact radius and indentation as a function of applied load.



APPENDIX IV - FINITE ELEMENT MODELLING

Problem Formulation

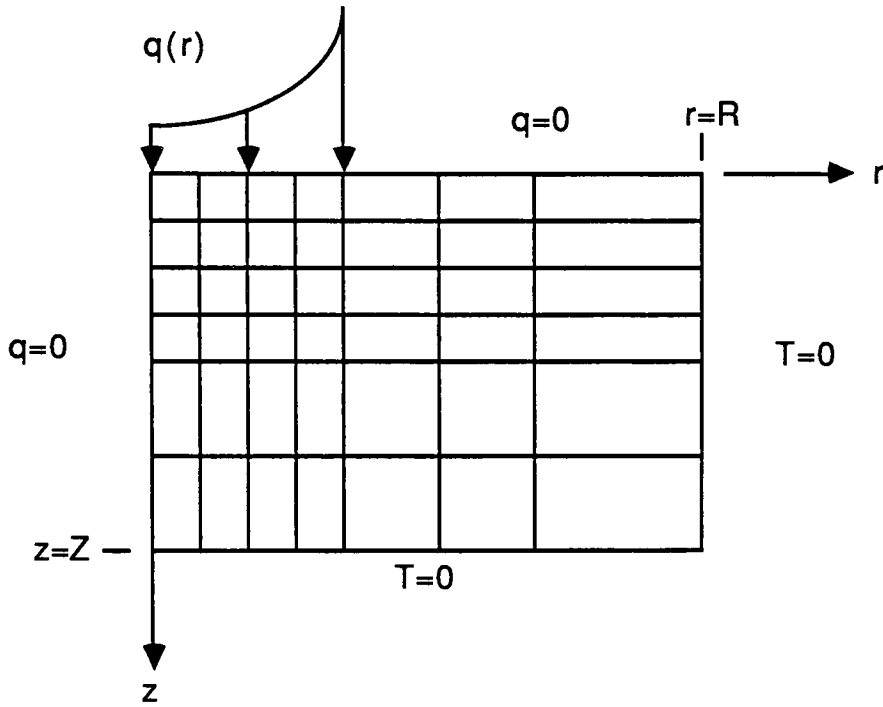


Figure IV.1
FEA domain

Given: Axially symmetric steady state heat flow into a cylindrical region of variable thermal conductivity.

Governing Equation:

$$\nabla \cdot (k \nabla T) = 0$$

Boundary conditions:

$$\frac{\partial T}{\partial r} (r=0) = 0$$

$$q(r) = \begin{cases} -k \frac{\partial T}{\partial z} & r < \hat{a} \\ 0 & r > \hat{a} \end{cases}$$

$$T (r=R) = T (z=Z) = 0$$

Weak formulation over an element:

$$0 = \int_{\Omega_e} \left[\nabla \cdot (k \nabla T) \right] v \, d\Omega$$

$$\int_{\Omega_e} \left[k \nabla T \cdot \nabla v \right] d\Omega = \iint_{\partial\Omega_e} q_n v \, dS$$

$$q_n = \hat{n} \cdot k \nabla T \quad \text{heat flux}$$

in cylindrical coordinates:

$$\int_{\Omega_e} \left[k \nabla T \cdot \nabla v \right] d\Omega = \int_{\Omega_e} k \left[\frac{\partial T}{\partial r} \hat{e}_r + \frac{1}{r} \frac{\partial T}{\partial \theta} \hat{e}_\theta + \frac{\partial T}{\partial z} \hat{e}_z \right] \cdot \left[\frac{\partial v}{\partial r} \hat{e}_r + \frac{1}{r} \frac{\partial v}{\partial \theta} \hat{e}_\theta + \frac{\partial v}{\partial z} \hat{e}_z \right] d\Omega$$

due to axial symmetry:

$$\frac{\partial T}{\partial \theta} = \frac{\partial v}{\partial \theta} = 0$$

therefore:

$$\int_{\Omega_e} \left[k \nabla T \cdot \nabla v \right] d\Omega = 2\pi \iint_{r,z} k \left[\frac{\partial T}{\partial r} \frac{\partial v}{\partial r} + \frac{\partial T}{\partial z} \frac{\partial v}{\partial z} \right] r \, dr dz$$

and:

$$2\pi \iint_{r,z} k \left[\frac{\partial T}{\partial r} \frac{\partial v}{\partial r} + \frac{\partial T}{\partial z} \frac{\partial v}{\partial z} \right] r \, dr dz = \iint_{\partial\Omega_e} q_n v \, dS$$

or:

$$B(v, T) = l(v)$$

Interpolation functions for a four noded-rectangular element:

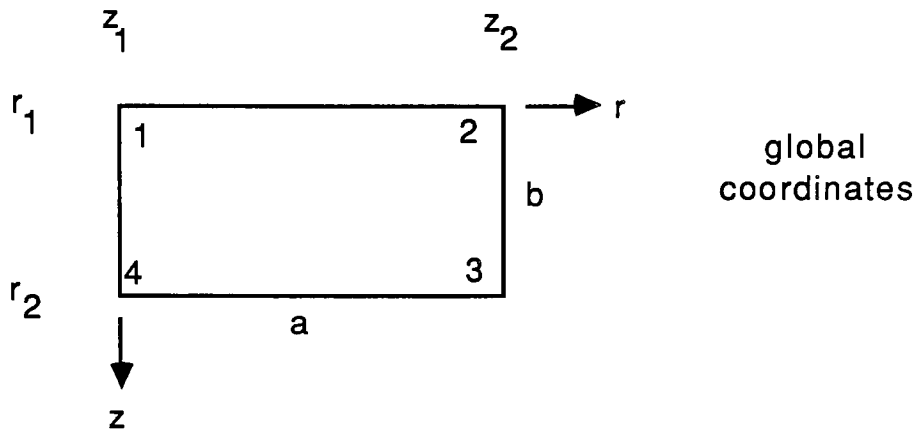


Figure IV.2
Shape functions

$$\psi_1(r,z) = \left[1 - \frac{r - r_1}{a} \right] \left[1 - \frac{z - z_1}{b} \right]$$

$$\psi_2(r,z) = \left[\frac{r - r_1}{a} \right] \left[1 - \frac{z - z_1}{b} \right]$$

$$\psi_3(r,z) = \left[\frac{r - r_1}{a} \right] \left[\frac{z - z_1}{b} \right]$$

$$\psi_4(r,z) = \left[1 - \frac{r - r_1}{a} \right] \left[\frac{z - z_1}{b} \right]$$

substitute:

$$T(r,z) = \sum_{j=1}^4 T_j \psi_j(r,z)$$

$$v(r,z) = \psi_i(r,z)$$

to get:

$$\sum_{j=1}^4 T_j B(\psi_i, \psi_j) = 1 (\psi_i)$$

$$K_{ij}^e = 2\pi \int_{r_1}^{r_2} \int_{z_1}^{z_2} k \left[\frac{\partial \psi_i}{\partial r} \frac{\partial \psi_j}{\partial r} + \frac{\partial \psi_j}{\partial z} \frac{\partial \psi_i}{\partial z} \right] r \, dr \, dz$$

$$F_i^e = \iint_{\partial \Omega_e} q_n \psi_i \, dS$$

To simplify integration, the following transformation is implemented:

$$T_e: \quad r = r_1 + a \xi \quad z = z_1 + b \eta$$

$$T_e^{-1}: \quad \xi = \frac{r - r_1}{a} \quad \eta = \frac{z - z_1}{b}$$

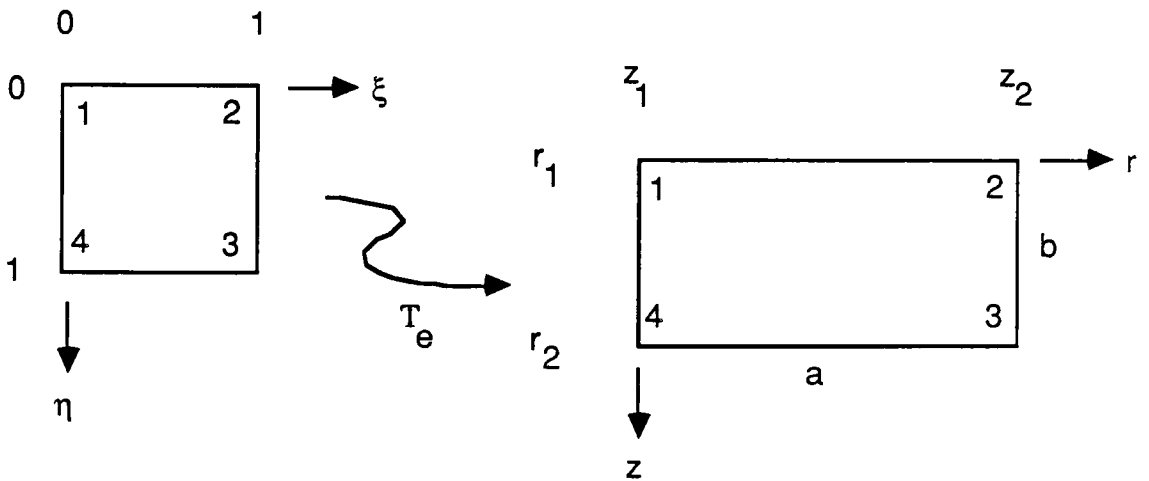


Figure IV.3
Coordinate transformation

The transformed interpolation functions are:

$$\phi_1 = (1 - \xi)(1 - \eta)$$

$$\phi_2 = \xi(1 - \eta)$$

$$\phi_3 = \xi\eta$$

$$\phi_4 = (1 - \xi)\eta$$

The element stiffness matrix terms are redefined as:

$$K_{ij}^e = 2\pi k \int_0^1 \int_0^1 \left[\frac{b}{a} \frac{\partial \phi_i}{\partial \xi} \frac{\partial \phi_j}{\partial \xi} + \frac{a}{b} \frac{\partial \phi_i}{\partial \eta} \frac{\partial \phi_j}{\partial \eta} \right] (r_1 + a\xi) d\xi d\eta$$

After integration, the element stiffness matrix is found to be symmetric about both diagonals. The individual terms are:

$$K_{11}^e = K_{44}^e = 2\pi k \left[\frac{r_1 b}{3a} + \frac{r_1 a}{3b} + \frac{b}{6} + \frac{a^2}{12b} \right]$$

$$K_{12}^e = K_{21}^e = K_{34}^e = K_{43}^e = 2\pi k \left[-\frac{r_1 b}{3a} + \frac{r_1 a}{3b} - \frac{b}{6} + \frac{a^2}{12b} \right]$$

$$K_{13}^e = K_{24}^e = K_{31}^e = K_{42}^e = 2\pi k \left[-\frac{r_1 b}{6a} - \frac{r_1 a}{6b} - \frac{b}{12} - \frac{a^2}{12b} \right]$$

$$K_{14}^e = K_{41}^e = 2\pi k \left[\frac{r_1 b}{6a} - \frac{r_1 a}{3b} + \frac{b}{12} - \frac{a^2}{12b} \right]$$

$$K_{22}^e = K_{33}^e = 2\pi k \left[\frac{r_1 b}{3a} + \frac{r_1 a}{3b} + \frac{b}{6} + \frac{a^2}{4b} \right]$$

In calculating the element force vector terms, it is convenient to classify the elements according to their boundaries. For this problem, three types of elements are present:

- A) Internal element or external element with prescribed zero heat flux over a surface.
- B) External element with prescribed non-zero heat flux over a surface.
- C) External element with prescribed temperature and unknown heat flux on a surface.

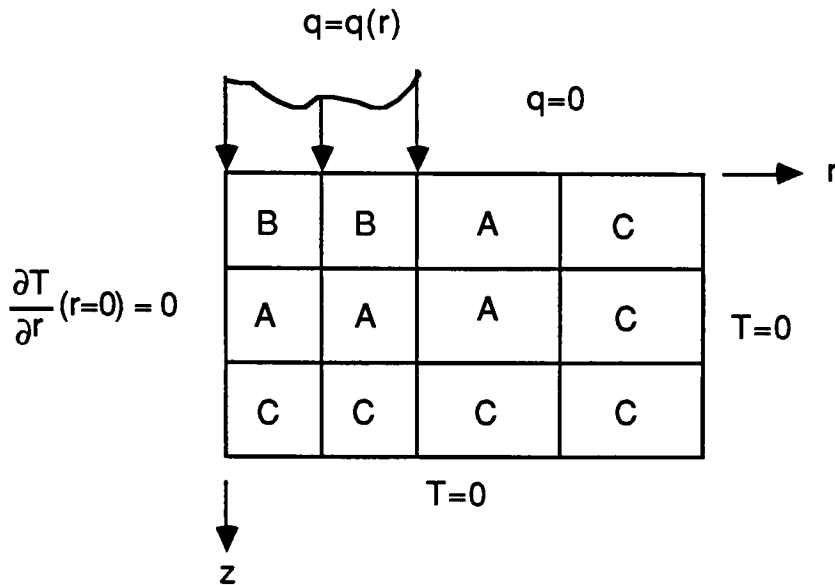


Figure IV.4
Element classification

The force vector terms for type A elements are zero, requiring no calculations. Type B elements must have the prescribed heat flux integrated against each shape function, resulting in non-zero terms. Zero temperature nodes are dropped from the global system of equations prior to their simultaneous solution for temperature. Therefore, type C elements require no force vector calculations. If need be, the heat flux from these elements can be found after the internal temperature distribution is established (not done in this case). The only force vector terms that need to be found are those of type B elements.

For this problem, the (non-zero) flux is prescribed over the $z=0$ surface, connecting nodes 1 and 2 of each element on this surface.

$$F_1^e = -2\pi k \int_{r_1}^{r_2} \frac{\partial T}{\partial z}(z=0) \left[1 - \frac{r - r_1}{a} \right] r \, dr$$

$$F_2^e = -2\pi k \int_{r_1}^{r_2} \frac{\partial T}{\partial z}(z=0) \left[\frac{r - r_1}{a} \right] r \, dr$$

The remaining two terms, 3 and 4, of each type B element force vector are zero (because the shape functions are zero at $z=0$).

For a bulk material, the flux profile resulting in a constant temperature over the surface of an element is [17]:

$$\frac{\partial T}{\partial z}(z=0) = \frac{-Q}{2\pi k \hat{a} (\hat{a}^2 - r^2)^{\frac{1}{2}}}$$

where Q is the power (rate of flow of heat) through the surface. The negative sign indicates heat is flowing into the region. The element force vector terms resulting from this heat flux profile are:

$$F_1^e = \frac{Q}{\hat{a}(r_2 - r_1)} \left[-\frac{r_2}{2} \sqrt{\hat{a}^2 - r_2^2} + \left[r_2 - \frac{r_1}{2} \right] \sqrt{\hat{a}^2 - r_1^2} - \frac{\hat{a}^2}{2} \left[\sin^{-1} \frac{r_2}{\hat{a}} - \sin^{-1} \frac{r_1}{\hat{a}} \right] \right]$$

$$F_2^e = \frac{Q}{\hat{a}(r_2 - r_1)} \left[\left[r_1 - \frac{r_2}{2} \right] \sqrt{\hat{a}^2 - r_2^2} - \frac{r_1}{2} \sqrt{\hat{a}^2 - r_1^2} + \frac{\hat{a}^2}{2} \left[\sin^{-1} \frac{r_2}{\hat{a}} - \sin^{-1} \frac{r_1}{\hat{a}} \right] \right]$$

Once all the element force and stiffness terms are calculated, the global force vector and stiffness matrix are assembled using a connectivity matrix [22]. The zero temperature terms are dropped, and the temperature at each element is found by Gaussian Elimination.

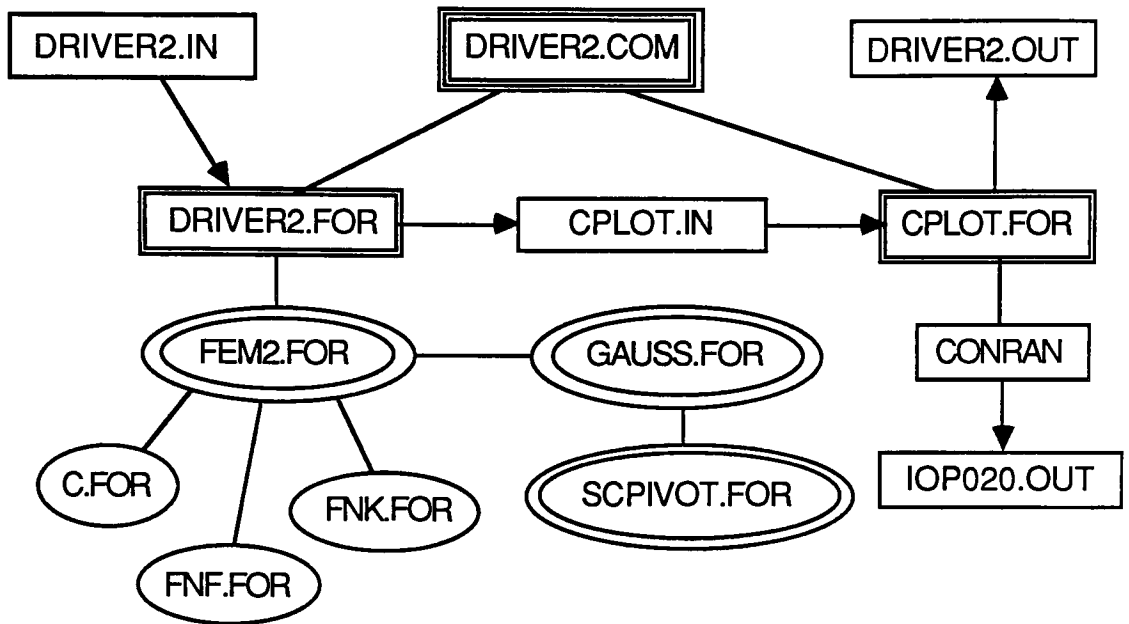


Figure IV.4
Finite element program map

The program package, shown graphically in Figure IV.4, is driven by a command file, and consists of two programs, four subroutines, and three function subprograms. The command file DRIVER2.COM directs the program DRIVER2.FOR to read the input data contained in DRIVER2.IN. FEM2.FOR is the main subroutine used for analysis. It calls the other other subroutines and functions in order to solve for the temperature distribution in the plate. The nodal coordiantes and temperatures are put into the output file CLOT.IN. The command file then directs the program CLOT.FOR to read this data as input. This program writes the temperature distribution along the flux surface, outputting it as DRIVER2.OUT, and calls the subroutine CONRAN from the library of subroutines accessible at RIT. CONRAN finds temperature contours, and creates a data plotting file IOP020.DAT.

The input data file consists of two sets of numbers: The number of coordinates in the 'r' direction, followed by the 'r' coordinates of the nodes, and the number of 'z' coordinates, followed by their values. The subroutine FEM2 automatically generates a grid of rectangular elements from these coordinates. The thermal conductivity, a function of both 'r' and 'z', is set in the function C.FOR. The input power, heat flow radius, and flux function are set in the function FNF.FOR.

Execution of the program package is straightforward. After logging on the VAX cluster, access must be gained to the NCAR plotting routine libraries. This is done by typing "@USER:[ENGLIB.VAXV]NCARDEFS.COM" at the dollar sign prompt. At this point, the two programs and their subprograms must be compiled and linked (no compilation is necessary for the NCAR routines). To execute the program, type "@DRIVER2". The temperature distribution along the $z=0$ surface will be output in the DRIVER2.OUT file, and the data for the contour plot will be stored in the IOP020.DAT file.

Tektronix mode is required to view the temperature contour plot. After logging on the VAX cluster, and accessing the NCAR library, type "PLOT". The cue "Meta option:" should appear on the monitor screen. At this point, type "Dev tt: 4010", followed by "read IOP020", and "plot". The screen should clear, and the plot should appear.

With some domain geometries, a plotting file is not created. For example, if the outer dimensions of the specimen are much larger than the flux circle, all the isotherms will be concentrated to a point, and no plot file will be created.

```
$ ASSIGN DRIVER2.IN FOR005  
$ ASSIGN CPLOT.IN FOR006  
$ RUN DRIVER2  
$ ASSIGN CPLOT.IN FOR005  
$ ASSIGN DRIVER2.OUT FOR006  
$ RUN CPLOT
```

```

*****
*
*   PROGRAM           :   DRIVER2
*
*   PROGRAMMER       :   C. AMSDEN
*
*   DATE WRITTEN    :   11 - 87
*
*   OBJECTIVE:
*       THIS PROGRAM IS INTENDED TO DRIVE THE SUBROUTINE
*       FEM2, WHICH USES THE FINITE ELEMENT METHOD TO SOLVE
*       FOR THE TEMPERATURE DISTRIBUTION IN A 2-D PLATE.
*
*   SUBPROGRAMS REFERENCED:
*       FEM2(MAXNR,MAXNZ,MAXN,MAXE,NR,NZ,NCR,NCZ,CONNECT,
*           ICOL,EK,EF,GK,GF,T)
*           SUBROUTINE WHICH SOLVES PROBLEM
*       C(R,Z)
*           FUNCTION WHICH SUPPLIES THERMAL CONDUCTIVITY
*           CALLED THROUGH FEM2
*       FNK(EI,EJ,A,B)
*           FUNCTION WHICH SUPPLIES ELEMENT STIFFNESS VALUES
*           CALLED THROUGH FEM2
*       FNF(I,R1,R2)
*           FUNCTION WHICH SUPPLIES FORCE VECTOR VALUES
*       GAUSS(MAXN,N,A,B,X,SUCCESS,ICOL)
*           SUBROUTINE WHICH USES GAUSSIAN ELIMINATION TO SOLVE
*           A SYSTEM OF EQUATIONS. CALLED THROUGH FEM2
*       SCPIVOT(MAXN,N,A,B,K,ICOL,SUCCESS)
*           SUBROUTINE TO SCALE AND COLUMN PIVOT AN AUGMENTED
*           MATRIX. CALLED THROUGH GAUSS
*
*   ARRAYS USED:
*       NCR   :   VECTOR OF R COORDINATES
*       NCZ   :   VECTOR OF Z COORDINATES
*       T     :   VECTOR OF NODE TEMPERATURES
*       EK    :   3-D MATRIX OF ELEMENT STIFFNESS VALUES
*       EF    :   2-D MATRIX OF ELEMENT FORCES
*       GK    :   2-D MATRIX OF GLOBAL STIFFNESS VALUES
*       GF    :   VECTOR OF GLOBAL FORCES
*       CONNECT : 2-D CONNECTIVITY MATRIX
*       ICOL  :   NODE RE-ORDER VECTOR
*
*   VARIABLES USED:
*       MAXNR :   MAXIMUM R COORDINATES TO BE INPUT
*       MAXNZ :   MAXIMUM Z COORDINATES TO BE INPUT
*       MAXN  :   MAXIMUM NODES = MAXNR * MAXNZ
*       MAXE  :   MAXIMUM ELEMENTS = (MAXNR-1) * (MAXNZ-1)
*       N     :   NUMBER OF NODES = NR * NZ
*       NR    :   NUMBER OF R COORDINATES
*       NZ    :   NUMBER OF Z COORDINATES
*
*****
*
*   PROGRAM DRIVER2
*
*   INTEGER MAXNR,MAXNZ,MAXN,MAXE
*   PARAMETER (MAXNR=30,MAXNZ=30,MAXN=900,MAXE=841)
*   INTEGER N,NR,NZ,CONNECT(MAXE,4),ICOL(MAXN)
*   REAL NCR(MAXNR),NCZ(MAXNZ),T(MAXN),EK(MAXE,4,4),EF(MAXE,4),

```

```

*      +      GK(MAXN,MAXN),GF(MAXN)
*
*      READ(5,*) NR
*      DO 100 J=1,NR
*          READ(5,*) NCR(J)
100     CONTINUE
*
*      READ(5,*) NZ
*      DO 200 I=1,NZ
*          READ(5,*) NCZ(I)
200     CONTINUE
*
*      +      CALL FEM2(MAXNR,MAXNZ,MAXN,MAXE,NR,NZ,NCR,NCZ,
*          CONNECT,ICOL,EK,EF,GK,GF,T)
*
*      N=NR*NZ
*      WRITE(6,10) NR,NZ
10      FORMAT(' ',I4,',',I4,',')
*
*      DO 300 I=1,NZ-1
*          DO 400 J=1,NR-1
*              K=(NR-1)*(I-1)+J
*              WRITE(6,20) NCR(J),NCZ(I),T(K)
20          FORMAT(' ',F12.6,',',F12.6,',',F12.6,',')
*              CONTINUE
400         WRITE(6,30) NCR(NR),NCZ(I),'00000.00000'
30         FORMAT(' ',F12.6,',',F12.6,',',A12,',')
*          CONTINUE
300
*      DO 500 J=1,NR
*          WRITE(6,30) NCR(J),NCZ(NZ),'00000.00000'
500     CONTINUE
*
*      STOP
*      END

```

```

*****
*
* SUBROUTINE : FEM2
*
* PROGRAMMER : C. AMSDEN
*
* DATE WRITTEN : 11 - 87
*
* OBJECTIVE:
* THIS SUBROUTINE USES THE FINITE ELEMENT METHOD TO
* SOLVE FOR THE TEMPERATURE DISTRIBUTION T(R,Z) IN A PLATE.
* 4-NODED RECTANGULAR ELEMENTS, AND LINEAR SHAPE FUNCTIONS
* ARE USED. THE HEAT FLUX AT Z=0 IS SPECIFIED AS A FUNCTION
* OF R. THE HEAT FLUX AT R=0 IS ZERO. THE REMAINING TWO
* BOUNDARIES HAVE ZERO TEMPERATURE. THE THERMAL CONDUCTIVITY
* IS CONSTANT OVER EACH ELEMENT, BUT MAY VARY GLOBALLY AS A
* FUNCTION OF BOTH R AND Z.
*
* SUBPROGRAMS REFERENCED:
* C(R,Z)
* THERMAL CONDUCTIVITY OF AN ELEMENT WITH LOCAL NODE 1
* AT (R,Z).
* FNK(EI,EJ,A,B,R1)
* FUNCTION WHICH SUPPLIES ELEMENT STIFFNESS VALUES.
* FNF(I,R1,R2)
* FUNCTION WHICH SUPPLIES FORCE VECTOR VALUES
* GAUSS(MAXN,N,A,B,X,SUCCESS,ICOL)
* SUBROUTINE WHICH SOLVES A SYSTEM OF SIMULTANEOUS
* ALGEBRAIC EQUATIONS USING GAUSSIAN ELIMINATION
* SCPIVOT(MAXN,N,A,B,K,ICOL,SUCCESS)
* SUBROUTINE WHICH SCALES AND COLUMN PIVOTS AN
* AUGMENTED MATRIX. CALLED THROUGH GAUSS.
*
* ARRAYS USED:
* NCR : VECTOR OF R COORDINATES
* NCZ : VECTOR OF Z COORDINATES
* T : VECTOR OF NODAL TEMPERATURES
* EK : 3-D MATRIX OF ELEMENT STIFFNESS VALUES
* EF : 2-D MATRIX OF ELEMENT FORCES
* GK : 2-D MATRIX OF GLOBAL STIFFNESS VALUES
* GF : VECTOR OF GLOBAL FORCES
* CONNECT : 2-D CONNECTIVITY MATRIX
* ICOL : NODE REORDER VECTOR
*
* VARIABLES USED:
* MAXNR : MAX NUMBER OF R COORDINATES
* MAXNZ : MAX NUMBER OF Z COORDINATES
* MAXN : MAX NUMBER OF NODES = MAXNR * MAXNZ
* MAXE : MAX NUMBER OF ELEMENTS=(MAXNR-1)*(MAXNZ-1)
* NR : NUMBER OF R COORDIANTES
* NZ : NUMBER OF Z COORDINATES
* N : NUMBER OF NODES
* E : NUMBER OF ELEMENTS
* EI : COUNTER
* EJ : COUNTER
* COND : ELEMENT THERMAL CONDUCTIVITY
* A : ELEMENT LENGTH IN R DIRECTION
* B : ELEMENT LENGTH IN Z DIRECTION
* R1 : R COORDINATE OF LOCAL NODE 1 OF ELEMENT
* R2 : R COORDINATE OF LOCAL NODE 2 OF ELEMENT

```

```

*          SUCCESS :          LOGICAL VARIABLE, PIVOTING SUCCESSFUL
*
*****
*
+   SUBROUTINE FEM2(MAXNR,MAXNZ,MAXN,MAXE,NR,NZ,NCR,NCZ,
+       CONNECT,ICOL,EK,EF,GK,GF,T)
*
+   INTEGER MAXNR,MAXNZ,MAXN,MAXE,NR,NZ,N,E,EI,EJ,
+       CONNECT(MAXE,4),ICOL(MAXN)
+   REAL NCR(MAXNR),NCZ(MAXNZ),T(MAXN),COND,EK(MAXE,4,4),EF(MAXE,4),
+       GK(MAXN,MAXN),GF(MAXN),A,B,R1,R2
*   LOGICAL*1 SUCCESS
*
+   EXTERNAL C,FNK,FNF
*
+   N=NR*NZ
+   E=(NR-1)*(NZ-1)
*
+   DO 100 I=1,N
+       GF(I)=0.0
+       DO 100 J=1,N
+           GK(I,J)=0.0
100  CONTINUE
*
+   DO 150 K=1,E
+       DO 150 I=1,4
+           EF(K,I)=0.0
+           DO 150 J=1,4
+               EK(K,I,J)=0.0
150  CONTINUE
*
+   DO 200 I=1,NZ-1
+       B=NCZ(I+1)-NCZ(I)
+       DO 200 J=1,NR-1
+           A=NCR(J+1)-NCR(J)
+           R1=NCR(J)
+           COND=C(NCR(J),NCZ(I))
+           K=(NR-1)*(I-1)+J
+           DO 200 EI=1,4
+               DO 200 EJ=1,4
+                   EK(K,EI,EJ)=COND*FNK(EI,EJ,A,B,R1)
200  CONTINUE
*
+   DO 300 J=1,NR-1
+       R1=NCR(J)
+       R2=NCR(J+1)
+
+       EF(J,1)=FNF(1,R1,R2)
+       EF(J,2)=FNF(2,R1,R2)
300  CONTINUE
*
+   DO 400 I=1,NZ-1
+       DO 400 J=1,NR-1
+           K=(NR-1)*(I-1)+J
+           CONNECT(K,1)=NR*(I-1)+J
+           CONNECT(K,2)=NR*(I-1)+J+1
+           CONNECT(K,3)=NR*I+J+1
+           CONNECT(K,4)=NR*I+J
400  CONTINUE
*

```

```

DO 500 I=1,N
DO 500 J=1,N
DO 500 K=1,E
DO 500 L=1,4
DO 500 M=1,4
IF ((CONNECT(K,L).EQ.I).AND.
(CONNECT(K,M).EQ.J)) THEN
GK(I,J)=GK(I,J)+EK(K,L,M)
ENDIF
+
500 CONTINUE
*
DO 550 I=1,N
DO 550 K=1,E
DO 550 L=1,4
IF (CONNECT(K,L).EQ.I) THEN
GF(I)=GF(I)+EF(K,L)
ENDIF
550 CONTINUE
*
DO 600 I=N,NR,-NR
DO 625 J=I,N-1
DO 650 K=1,I-1
GK(J,K)=GK(J+1,K)
GK(K,J)=GK(K,J+1)
650 CONTINUE
DO 675 K=I,N-1
GK(J,K)=GK(J+1,K+1)
675 CONTINUE
GF(J)=GF(J+1)
625 CONTINUE
N=N-1
600 CONTINUE
N=N-(NR-1)
*
CALL GAUSS(MAXN,N,GK,GF,T,SUCCESS,ICOL)
IF (.NOT.SUCCESS) THEN
WRITE(6,10)
10 FORMAT('0','GAUSSIAN ELIMINATION UNSUCCESSFUL, ZERO ROW, ',
+ 'EXECUTION TERMINATED')
STOP
ENDIF
*
RETURN
END

```

```

*****
*
*   FUNCTION           :           C
*
*   PROGRAMMER        :           C. AMSDEN
*
*   DATE WRITTEN     :           11 - 87
*
*   PURPOSE:
*           THIS FUNCTION SUPPLIES THERMAL CONDUCTIVITIES, WHICH
*           MAY VARY WITH R AND Z
*
*****
*
*   REAL FUNCTION C(R,Z)
*
*   REAL R,Z
*
*   IF (Z.LT..125) THEN
*       C=5.0
*       RETURN
*   ENDIF
*
*   C=35.0
*
*   RETURN
*   END

```



```

*****
*
*   FUNCTION       :       FNF
*
*   PROGRAMMER    :       C. AMSDEN
*
*   DATE WRITTEN  :       11 - 87
*
*   PURPOSE:
*       THIS FUNCTION SUPPLIES PRE-INTEGRATED EQUATIONS REPRESENTING
*       A CONSTANT TEMPERATURE HEAT FLUX INTEGRATED AGAINST LINEAR,
*       FOUR-NODED INTERPOLATION FUNCTIONS.
*
*   VARIABLES USED:
*       R1       :       LOCAL NODE 1 GLOBAL COORDINATE
*       R2       :       LOCAL NODE 2 GLOBAL COORDINATE
*       AG       :       BOUNDARY LOCATION - FLUX DISCONTINUOUS
*       Q        :       POWER (IN - POSITIVE, OUT - NEGATIVE)
*       I        :       SHAPE FUNCTION USED
*****
*
REAL FUNCTION FNF(I,R1,R2)
*
INTEGER I
REAL R1,R2,AG,Q
*
Q=100.0
AG=.00018
*
IF (R2.LE.AG) THEN
1   GOTO (1,2),I
    FNF=Q*((-.5*R2*SQRT(AG**2-R2**2))
+         +((R2-.5*R1)*SQRT(AG**2-R1**2))
+         -((.5*AG**2)*(ASIN(R2/AG)-ASIN(R1/AG))))
+         /(AG*(R2-R1))
    RETURN
2   FNF=Q*((-.5*R1*SQRT(AG**2-R1**2))
+         +((R1-.5*R2)*SQRT(AG**2-R2**2))
+         -((.5*AG**2)*(ASIN(R1/AG)-ASIN(R2/AG))))
+         /(AG*(R2-R1))
    RETURN
ENDIF
*
FN=0.0
*
RETURN
END

```

```

*****
*
*   FUNCTION           :           FNK
*
*   PROGRAMMER        :           C. AMSDEN
*
*   DATE WRITTEN      :           11 - 87
*
*   PURPOSE:
*   THIS FUNCTION SUPPLIES ELEMENT STIFFNESS VALUES FOR 4-NODED
*   RECTANGULAR ELEMENTS, USING LINEAR SHAPE FUNCTIONS
*
*****
*
REAL FUNCTION FNK(EI,EJ,A,B,R1)
*
INTEGER EI,EJ,P
REAL A,B,R1
*
P=10*EI+EJ
*
IF ((P.EQ.11).OR.(P.EQ.44)) THEN
    FNK=(R1*B/(3.0*A))+(R1*A/(3.0*B))+(B/6.0)+(A**2/(12.0*B))
ELSEIF ((P.EQ.12).OR.(P.EQ.21).OR.(P.EQ.34).OR.(P.EQ.43)) THEN
    FNK=-(R1*B/(3.0*A))+(R1*A/(6.0*B))-(B/6.0)+(A**2/(12.0*B))
ELSEIF ((P.EQ.13).OR.(P.EQ.31).OR.(P.EQ.24).OR.(P.EQ.42)) THEN
    FNK=-(R1*B/(6.0*A))-(R1*A/(6.0*B))-(B/12.0)-(A**2/(12.0*B))
ELSEIF ((P.EQ.14).OR.(P.EQ.41)) THEN
    FNK=(R1*B/(6.0*A))-(R1*A/(3.0*B))+(B/12.0)-(A**2/(12.0*B))
ELSEIF ((P.EQ.22).OR.(P.EQ.33)) THEN
    FNK=(R1*B/(3.0*A))+(R1*A/(3.0*B))+(B/6.0)+(A**2/(4.0*B))
ELSEIF ((P.EQ.32).OR.(P.EQ.23)) THEN
    FNK=(R1*B/(6.0*A))-(R1*A/(3.0*B))+(B/12.0)-(A**2/(4.0*B))
ENDIF
*
FNK=FNK*6.28318
*
RETURN
END

```

```

*****
*
*   SUBROUTINE      :      GAUSS
*
*   PROGRAMMER     :      C. AMSDEN
*
*   DATE WRITTEN   :      7 - 86
*
*   OBJECTIVE:
*       THE OBJECTIVE OF THIS SUBROUTINE IS TO PERFORM GAUSSIAN
*       ELIMINATION ON A SYSTEM OF NON-HOMOGENEOUS LINEAR
*       ALGEBRAIC EQUATIONS. SCALING AND COLUMN PIVOTING ARE
*       DONE PRIOR TO THE ELIMINATION PROCESS.
*
*   USAGE:
*       GAUSS(MAXN,N,A,B,X,SUCCESS,ICOL)
*
*   SUBPROGRAMS REFERENCED:
*       SCPIVOT(MAXN,N,A,B,K,ICOL,SUCCESS)
*       SUBPROGRAM TO SCALE AND COLUMN PIVOT A GIVEN ROW
*
*   VARIABLES USED:
*       MAXN      :      ARRAY BOUND
*       I         :      ROW INDICATOR
*       J         :      COLUMN INDICATOR
*       K         :      WORKING VARIABLE
*       M         :      MULTIPLIER
*       SUM       :      CUMULATIVE TOTAL
*       SUCCESS   :      FLAG TO DENOTE SUCCESSFUL COMPLETION
*
*   ARRAYS USED:
*       ICOL      :      RECORDS COLUMN PIVOTS
*       A         :      EQUATION COEFFICIENTS
*       B         :      RESIDUALS
*       X         :      SOLUTIONS
*
*   SUBROUTINE GAUSS(MAXN,N,A,B,X,SUCCESS,ICOL)
*
*   INTEGER*4 ICOL(MAXN),I,J,K
*   REAL*4 A(MAXN,MAXN),B(MAXN),X(MAXN),M,SUM
*   LOGICAL*1 SUCCESS
*
*   SUCCESS=.FALSE.
*
*   DO 100 K=1,N-1
*       CALL SCPIVOT(MAXN,N,A,B,K,ICOL,SUCCESS)
*
*       IF (A(K,K).EQ.0) THEN                !PIVOT EACH ROW
*           SUCCESS=.FALSE.                 !FALSE INDICATES
*       ENDIF                                !UNSUCCESSFUL PIVOTING
*
*       IF (SUCCESS.EQ..FALSE.) THEN
*           RETURN
*       ENDIF
*
*       DO 200 I=K+1,N
*           M=A(I,K)/A(K,K)
*
*           DO 300 J=K,N                      !GAUSSIAN

```

```

300             A(I,J)=A(I,J)-M*A(K,J) !ELIMINATION ON
*             CONTINUE                !EACH ROW
200             B(I)=B(I)-M*B(K)
*             CONTINUE
100             CONTINUE
*
DO 400 I=N,1,-1
    SUM=0.0
*
    DO 500 K=I+1,N
        SUM=SUM+A(I,K)*X(ICOL(K))
        !BACK SUBSTITUTE
        !AND REORDER TO
        !OBTAIN SOLUTIONS
500     CONTINUE
*
400     X(ICOL(I))=(B(I)-SUM)/A(I,I)
*     CONTINUE
*
    SUCCESS=.TRUE.
*
    RETURN
    END

```

```

*****
*
*      SUBROUTINE      :      SCPIVOT
*
*      PROGRAMMER      :      C. AMSDEN
*
*      DATE WRITTEN    :      7 - 86
*
*      OBJECTIVE:
*          THE OBJECTIVE OF THIS SUBROUTINE IS TO SCALE AND COLUMN
*          PIVOT A GIVEN ROW OF AN ARRAY
*
*      USAGE:
*          SCPIVOT(MAXN,N,A,B,K,ICOL,SUCCESS)
*
*      SUBROUTINES REFERENCED:
*          NONE
*
*      VARIABLES USED:
*          MAXN      :      ARRAY BOUND
*          ISWITCH   :      SWITCHING VARIABLE
*          I         :      ROW INDICATOR
*          J         :      COLUMN INDICATOR
*          K         :      ROW BEING WORKED ON
*          SCALE     :      SCALE FACTOR
*          JMAX      :      COLUMN WITH LARGEST VALUE
*          SWITCH    :      SWITCHING VARIABLE
*          SUCCESS   :      FLAG TO DENOTE SUCCESSFUL COMPLETION
*
*      ARRAYS USED:
*          ICOL      :      RECORDS COLUMN EXCHANGES
*          A         :      EQUATION COEFFICINTS
*          B         :      RESIDUALS
*
*      SUBROUTINE SCPIVOT(MAXN,N,A,B,K,ICOL,SUCCESS)
*
*      INTEGER*4 ICOL(MAXN),ISWITCH,I,J,K
*      REAL*4 A(MAXN,MAXN),B(MAXN),SCALE,JMAX,SWITCH
*      LOGICAL*1 SUCCESS
*
*      IF (K.EQ.1) THEN
*          DO 100 I=1,N                !INITIALIZE ICOL VALUES
*              ICOL(I)=I
*          CONTINUE
100      ENDIF
*
*      JMAX=K                          !ASSUME DIAGONAL LARGEST
*
*      DO 200 J=K+1,N
*          IF (ABS(A(K,J)).GT.ABS(A(K,JMAX))) THEN
*              JMAX=J
*          ENDIF                        !DENOTE LARGER VALUE
*
200      CONTINUE
*
*      IF (A(K,JMAX).EQ.0) THEN
*          SUCCESS=.FALSE.             !RETURN IF ALL COEFFICIENTS ZERO
*          RETURN
*      ENDIF

```

```

*
*   SCALE=A(K,JMAX)           !DEFINE SCALE FACTOR
*
DO 300 J=K,N
  A(K,J)=A(K,J)/SCALE        !SCALE COEFFICIENTS
300 CONTINUE
*
  B(K)=B(K)/SCALE           !SCALE RESIDUALS
*
  IF (JMAX.NE.K) THEN
    DO 400 I=1,N
      SWITCH=A(I,K)
      A(I,K)=A(I,JMAX)       !PERFORM PIVOTING
      A(I,JMAX)=SWITCH
400 CONTINUE
*
      ISWITCH=ICOL(JMAX)
      ICOL(JMAX)=ICOL(K)     !RECORD PIVOTING
      ICOL(K)=ISWITCH
    ENDIF
*
    SUCCESS=.TRUE.
*
    RETURN
    END

```

```

*****
*
*   PROGRAM       :       CPLOT
*
*   PROGRAMMER    :       C. AMSDEN
*
*   DATE WRITTEN  :       1 - 88
*
*   OBJECTIVE:
*       THIS PROGRAM PLOTS THE OUTPUT DATA OF A 2-D FINITE ELEMENT
*       PROGRAM, WHICH SOLVES FOR THE TEMPERATURE DISTRIBUTION IN A
*       CYLINDRICAL DOMAIN. CONTOUR PLOTTING IS PERFORMED BY
*       SUBROUTINES WRITTEN BY THE NATIONAL CENTER FOR ATMOSPHERIC
*       RESEARCH (NCAR). PLOTS MUST BE VIEWED ON A TEKTRONIX 4010
*       TERMINAL. FOR MORE INFORMATION, CONSULT THE NCAR MANUAL.
*
*   SUBROUTINES REFERENCED:
*       CONRAN(NCR,NCZ,T,N,WK,IWK,SCRARR)
*       NCAR CONTOUR PLOT SUBROUTINE
*
*   ARRAYS USED:
*       NCR       :       DATA COORDINATE   R
*       NCZ       :       DATA COORDINATE - Z
*       T         :       TEMPERATURE
*       WK        \
*       IWK       >       WORK ARRAYS
*       SCRARR    /
*
*   VARIABLES USED:
*       MAXN      :       MAXIMUM DATA POINTS (PARAMETER)
*       NCP       :       WORK ARRAY PARAMETER
*       RESOLUTION :       VIEW PARAMETER
*       N         :       NUMBER OF DATA POINTS = NR*NZ
*       NR        :       NUMBER OF R COORDINATES
*       NZ        :       NUMBER OF Z COORDINATES
*
*****
*
*   PROGRAM CPLOT
*
*   INTEGER MAXN,NCP,RESOLUTION
*   PARAMETER (MAXN=900,NCP=4,RESOLUTION=40)
*   REAL NCR(MAXN),NCZ(MAXN),T(MAXN),WK(13*MAXN)
*   INTEGER N,NR,NZ,IWK((27+NCP)*MAXN),SCRARR(RESOLUTION**2)
*
*   READ(5,*) NR,NZ
*
*   N=NR*NZ
*   DO 100 I=1,N
*     READ(5,*) NCR(I),NCZ(I),T(I)
100  CONTINUE
*
*   WRITE(6,10)
10  FORMAT('0',10X,'TEMPERATURE OVER THE FLUX SURFACE',/,
+      11X,'R',16X,'Z',15X,'T',/,10X,<37>(' - '))
*
*   DO 200 I=1,NR
*     WRITE(6,20) NCR(I),NCZ(I),T(I)
20  FORMAT(' ',7X,F8.5,8X,F8.5,7X,F9.4)
200  CONTINUE

```

```
*  
* CALL CONRAN(NCR,NCZ,T,N,WK,IWK,SCRARR)  
*  
STOP  
END
```


APPENDIX V - DERIVATION OF THE THERMAL CONSTRICTION RESISTANCE

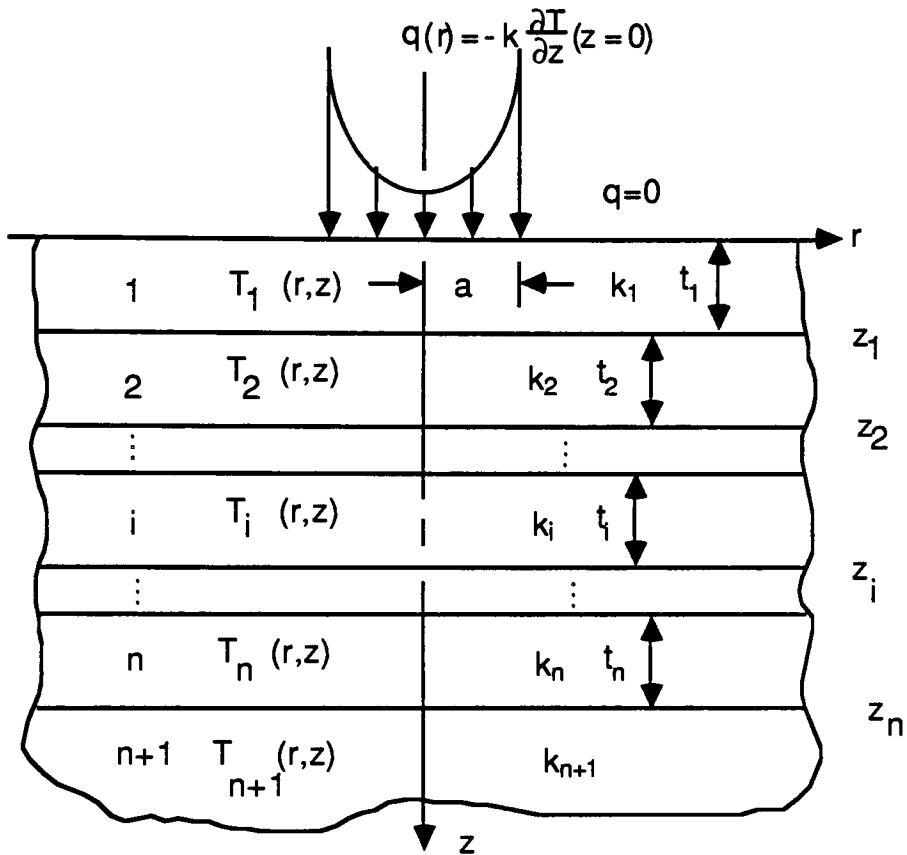


Figure V.1
TCR derivation domain

Given: Axially symmetric heat flow through a circular spot of radius 'a' into an infinite half-space with 'n' surface coatings of thickness t_i , and thermal conductivity k_i ($i = 1, 2, 3, \dots, n$).

Governing equations:

$$\frac{\partial^2 T_i}{\partial r^2} + \frac{1}{r} \frac{\partial T_i}{\partial r} + \frac{\partial^2 T_i}{\partial z^2} = 0, \quad z_{i-1} < z < z_i, \quad i = 1, 2, 3, \dots, n$$

$$\frac{\partial^2 T_{n+1}}{\partial r^2} + \frac{1}{r} \frac{\partial T_{n+1}}{\partial r} + \frac{\partial^2 T_{n+1}}{\partial z^2} = 0, \quad z > z_n$$

Boundary conditions:

$$q(r) = \begin{cases} -k_1 \frac{\partial T_1}{\partial z}(z=0) & r < a \\ 0 & r > a \end{cases}$$

$$\frac{\partial T}{\partial r}(r=0) = 0$$

$$\left. \begin{array}{l} T_i = T_{i+1} \\ k_i \frac{\partial T_i}{\partial z} = k_{i+1} \frac{\partial T_{i+1}}{\partial z} \end{array} \right\} z = z_i, \quad i = 1, 2, 3, \dots, n$$

$T = 0$ as 'r' and 'z' go to infinity

This formulation consists of 'n+1' boundary value problems, coupled through the boundary conditions. The equations can be solved for the temperature in each region by implementing the Hankel transform of order zero [15,17,27]. The transformed variables are:

$$T_i^*(\zeta, z) = A_i(\zeta) e^{\zeta z} + B_i(\zeta) e^{-\zeta z}$$

$$T_{n+1}^*(\zeta, z) = C(\zeta) e^{-\zeta z}$$

A_i , B_i , and C are found by applying the boundary conditions. This allows the determination of T_1^* . Taking the inverse transform:

$$T_1(r,z) = \int_{\zeta=0}^{\infty} \zeta T_1^*(\zeta,z) J_0(\zeta r) d\zeta$$

The average temperature over the flux surface is:

$$T_m = \frac{2}{a^2} \int_0^a T_1(r,0) r dr$$

Thus, the thermal constriction resistance can be defined:

$$R = \frac{T_m}{Q}$$

where 'Q' is the rate of heat flow (power) through the circular spot.

This thermal constriction resistance could be used to determine the thermal conductivity of a single film in a multilayer stack of 'n' films. All the film thermal conductivities but one must be known. Caution must be exercised, however. If there is error in the assumed film conductivities, it would propagate as error in the film conductivity solved for.